ARTICLE

doi:10.1016/j.ymthe.2005.11.010

A Histone Deacetylase Inhibitor Enhances Recombinant Adeno-associated Virus-Mediated Gene Expression in Tumor Cells

Takashi Okada,[1,*] Ryosuke Uchibori,[1] Mayumi Iwata-Okada,[2] Masafumi Takahashi,[3] Tatsuya Nomoto,[1] Mutsuko Nonaka-Sarukawa,[1] Takayuki Ito,[1] Yuhe Liu,[1] Hiroaki Mizukami,[1] Akihiro Kume,[1] Eiji Kobayashi,[3] and Keiya Ozawa[1,2]

[1]*Division of Genetic Therapeutics,* [3]*Division of Organ Replacement Research, Center for Molecular Medicine, and* [2]*Division of Hematology, Department of Medicine, Jichi Medical School, Tochigi 329-0498, Japan*

**To whom correspondence and reprint requests should be addressed at the Division of Genetic Therapeutics, Center for Molecular Medicine, Jichi Medical School, 3311-1 Yakushiji, Minami-Kawachi, Tochigi 329-0498, Japan. Fax: +81 285 44 8675. E-mail: tokada@jichi.ac.jp.*

Available online 4 January 2006

The transduction of cancer cells using recombinant adeno-associated virus (rAAV) occurs with low efficiency, which limits its utility in cancer gene therapy. We have previously sought to enhance rAAV-mediated transduction of cancer cells by applying DNA-damaging stresses. In this study, we examined the effects of the histone deacetylase inhibitor FR901228 on tumor transduction mediated by rAAV types 2 and 5. FR901228 treatment significantly improved the expression of the transgene in four cancer cell lines. The cell surface levels of alpha v integrin, FGF-R1, and PDGF-R were modestly enhanced by the presence of FR901228. These results suggest that the superior transduction induced by the HDAC inhibitor was due to an enhancement of transgene expression rather than increased viral entry. Furthermore, we characterized the association of the acetylated histone H3 in the episomal AAV vector genome by using the chromatin immunoprecipitation assay. The results suggest that the superior transduction may be related to the proposed histone-associated chromatin form of the rAAV concatemer in transduced cells. In the analysis with subcutaneous tumor models, strong enhancement of the transgene expression as well as therapeutic effect was confirmed *in vivo*. The use of this HDAC inhibitor may enhance the utility of rAAV-mediated transduction strategies for cancer gene therapy.

Key Words: histone deacetylase inhibitor, AAV vector, cancer

INTRODUCTION

Recombinant adeno-associated virus (rAAV) has been of considerable interest to developers of clinical gene therapies [1,2]. This is because, unlike adenoviruses, the introduction of AAV vectors has not been associated with significant inflammation either experimentally or clinically [3]. Furthermore, diseases associated with AAV have not been found in human or animal populations. However, the transduction of cancer cells using rAAV occurs with very low efficiency, which limits its utility in gene therapy. Consequently, we have sought to enhance rAAV-mediated transduction of cancer cells by applying DNA-damaging stresses such as γ-rays or anticancer agents [4–6].

An alternative approach to improving the rAAV-mediated transduction of tumor cells may be to enhance transcription in the target cells. One technique to bring about this event may be to apply a histone deacetylase (HDAC) inhibitor, since HDAC inhibitors are known to regulate the transcription of various genes. Significantly, an HDAC inhibitor increases adenovirus-mediated transduction of cancer cell lines because it enhances the levels of the viral receptor on the cell surface [7]. On the other hand, the effects of HDAC inhibitors on rAAV-mediated transduction of tumor cells have not yet been fully elucidated. Treatment with an HDAC inhibitor causes gene expression from a silenced rAAV genome that has been integrated into the host's genome to recover [8]. However, rAAV exists mostly as an extrachromosomal genome rather than as an integrated genome, and this extrachromosomal form is the primary source of rAAV-mediated gene expression [9]. Therefore, the HDAC inhibitor-mediated recovery of expression from the integrated and silenced genome does not reflect a typical situation of rAAV-mediated transduction. Whereas no

1525-0016/$30.00

clear mechanism has been determined for the effect on the episomal vector-mediated expression, the histone deacetylase inhibitor should also contribute to the enhanced transcription before integration occurs.

Here we show that HDAC inhibitors markedly enhance the transgene expression immediately after rAAV-mediated transduction of tumor cells *in vitro* as well as *in vivo*. Our data also suggest that the vector genome in the cells is in the histone-associated chromatin form, which is capable of superior transcription. HDAC inhibitors may improve tumor cell transduction by enhancing the acetylation of the histone-associated chromatin of the rAAV genome.

RESULTS

Effects of FR901228 Treatment on the Transduction of U251MG Cells with rAAV

To analyze whether an HDAC inhibitor can also improve rAAV-mediated gene expression soon after the infection,

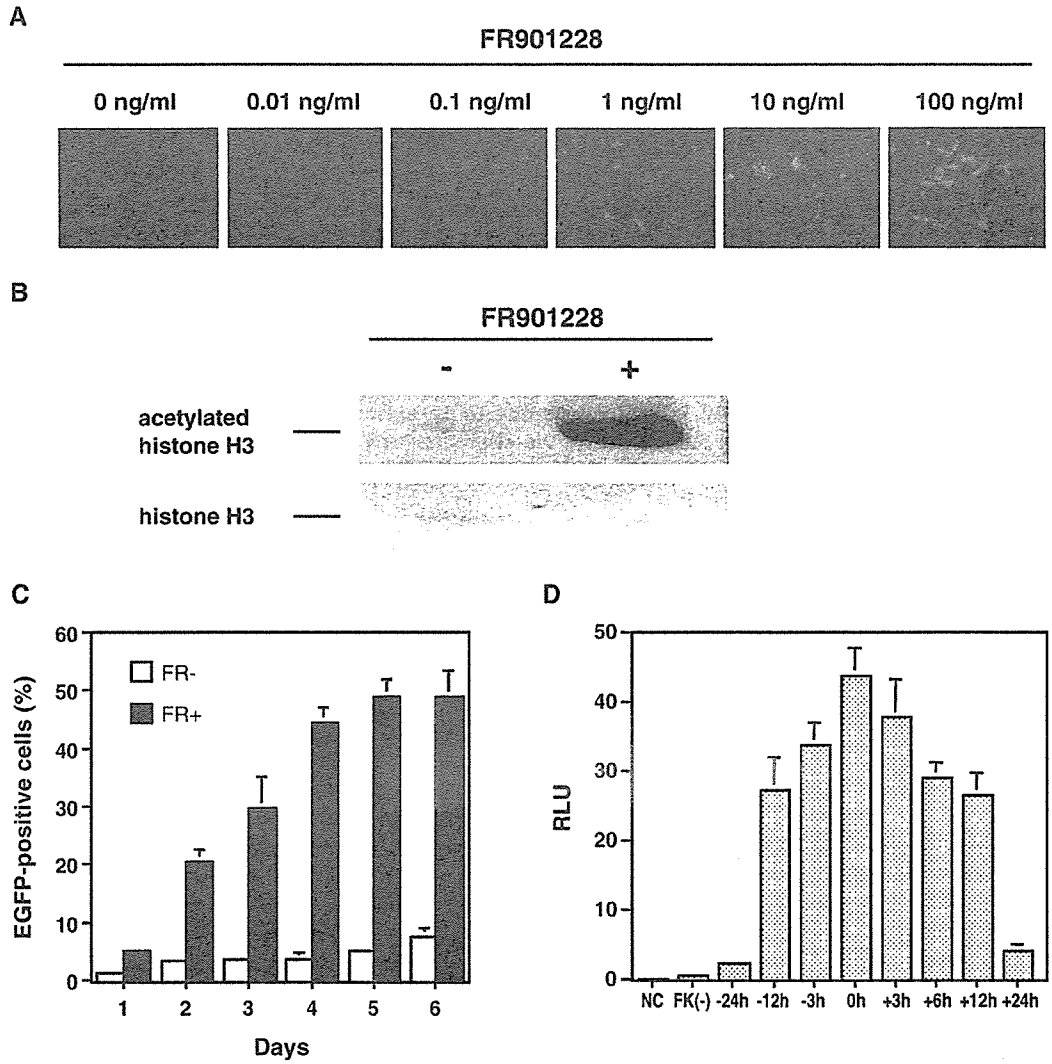

FIG. 1. (A) Effects of FR901228 treatment on the transduction of U251MG cells with rAAV. U251MG cells were infected with 1×10^4 genome copies/cell of AAV2EGFP in the presence of various concentrations of FR901228. EGFP expression was observed 24 h after infection. (B) Detection of the histone acetylation in U251MG cells caused by FR901228 treatment. Cells were incubated in the presence or absence of FR901228 for 24 h. The levels of acetylated histone H3 and histone H3 were determined by Western blot analysis. Histone H3 serves as a loading control. (C) The percentage of EGFP-positive cells at various time points after transduction with AAV2EGFP in the presence (FR+) or absence (FR−) of 1 ng/ml FR901228 was determined by FACS. Cells were infected with AAV2EGFP at 1×10^3 genome copies/cell. The data shown are the means and standard deviations of three independent experiments. (D) The kinetics of the effect on the FR901228-assisted transduction of U251MG cells. Cells were treated with FR901228 at various time points around the transduction with rAAV expressing luciferase as indicated. Luciferase assay was performed on the luminometer 48 h after the transduction.

doi:10.1016/j.ymthe.2005.11.010

we transduced U-251MG human glioma cells with EGFP-expressing rAAV (AAV2EGFP) in the presence of the HDAC inhibitor FR901228. We found that FR901228 treatment improved the AAV2EGFP-mediated gene expression in a dose-dependent manner early after the infection (Fig. 1A). The fact that FR901228 also enhanced the acetylation of the histones in the cells was confirmed by Western blot analysis (Fig. 1B). To assess when gene expression was maximal, we transduced U251MG cells with AAV2EGFP in the presence or absence of 1 ng/ml FR901228 and assessed EGFP expression at various time points after transduction (Fig. 1C). This revealed that the enhancement of gene expression depended on the incubation period and required 4 days before the expression reach a plateau. To analyze the kinetics of the effect on the FR901228-assisted transduction of U251MG cells, cells were treated with FR901228 at various time points around the transduction with luciferase-expressing rAAV type 2 (AAV2-Luc) (Fig. 1D). As a result, the transduction efficiency peaked when cells were treated with FR901228 at the time of virus transduction.

TABLE 1: Relative expression of FGF-R1 and PDGF-R in U251MG cells treated with recombinant AAV alone (1×10^4 genome copies/cell) or together with FR901228 (0.3 or 3 ng/ml) for 24 h as analyzed by quantitative PCR

	$2^{\text{correctedΔCt (GAPDH – target)}}$	
FR901228 (ng/ml)	FGF-R1	PDGF-Rα
0	1.00	1.00
0.3	1.28	1.77
3	1.60	2.30

The relative expression of the target mRNA was determined as the ratio of the expression in U251MG cells treated with recombinant AAV and FR901228 to that in U251MG cells treated with recombinant AAV alone. Data are means ($n = 5$).

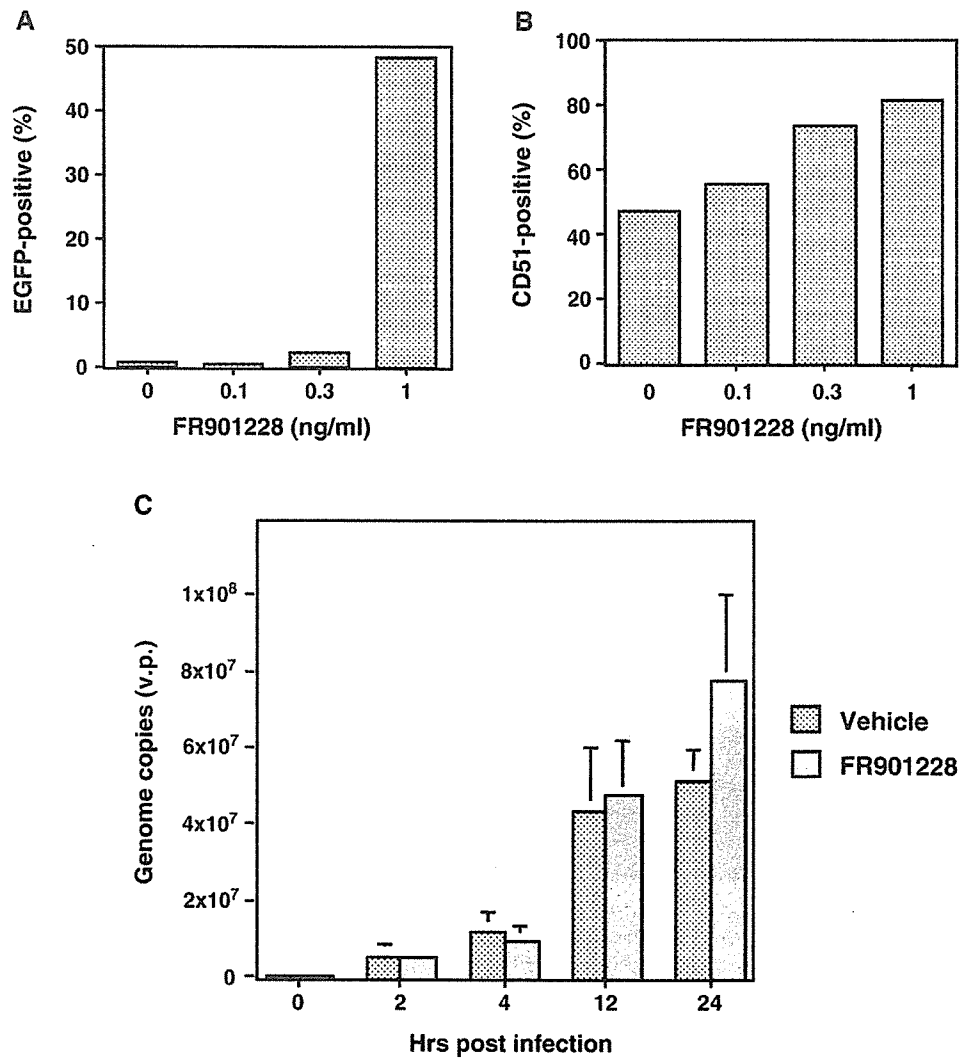

FIG. 2. (A) Percentage of EGFP-positive U251MG cells after transduction with 1×10^4 genome copies/cell of AAV2EGFP in the presence of various concentrations of FR901228. The cells were analyzed 24 h after the transduction for EGFP expression by FACS. The data shown are the average percentages of EGFP-positive cells after three independent transductions. (B) Integrin expression in transduced cells is only modestly enhanced by FR901228 treatment. The cells were stained 24 h after the transduction with monoclonal antibodies to CD51 (integrin v chain, clone 13C2) and analyzed by FACS. The data shown are the average percentages of positive cells after three independent transductions. (C) Transgene copy number in U251MG cells transduced with 1×10^4 genome copies/cell of AAV2EGFP in the presence of 1 ng/ml FR901228. The copy number of the transgene was estimated by real-time PCR at 0, 2, 4, 12, and 24 h after the rAAV infection.

Effects on Receptor Expression and Viral Entry

To determine if FR901228 acted by enhancing the entry of rAAV, we infected U251MG cells with AAV2EGFP in the presence of various concentrations of FR901228 and then analyzed the EGFP and alpha v integrin levels in the cells by fluorescence-activated cell sorting (FACS). This analysis showed that 24 h after AAV2EGFP infection with 1 ng/ml FR901228, 48% of the U251MG cells were EGFP-positive, whereas at lower concentrations of FR901228 only very few cells were EGFP-positive (Fig. 2A). However, this FR901228 concentration range (0.3–1 ng/ml) only modestly enhanced the levels of AAV2 coreceptor, alpha v integrin (Fig. 2B). In addition, when we estimated the amount of the rAAV genome in the transduced cells by real-time quantitative PCR analysis, we found that FR901228 treatment did not significantly affect the copy number of the rAAV (Fig. 2C). Furthermore, we also estimated the effect of FR901228 on the expression of coreceptors for the AAV. FR901228 moderately

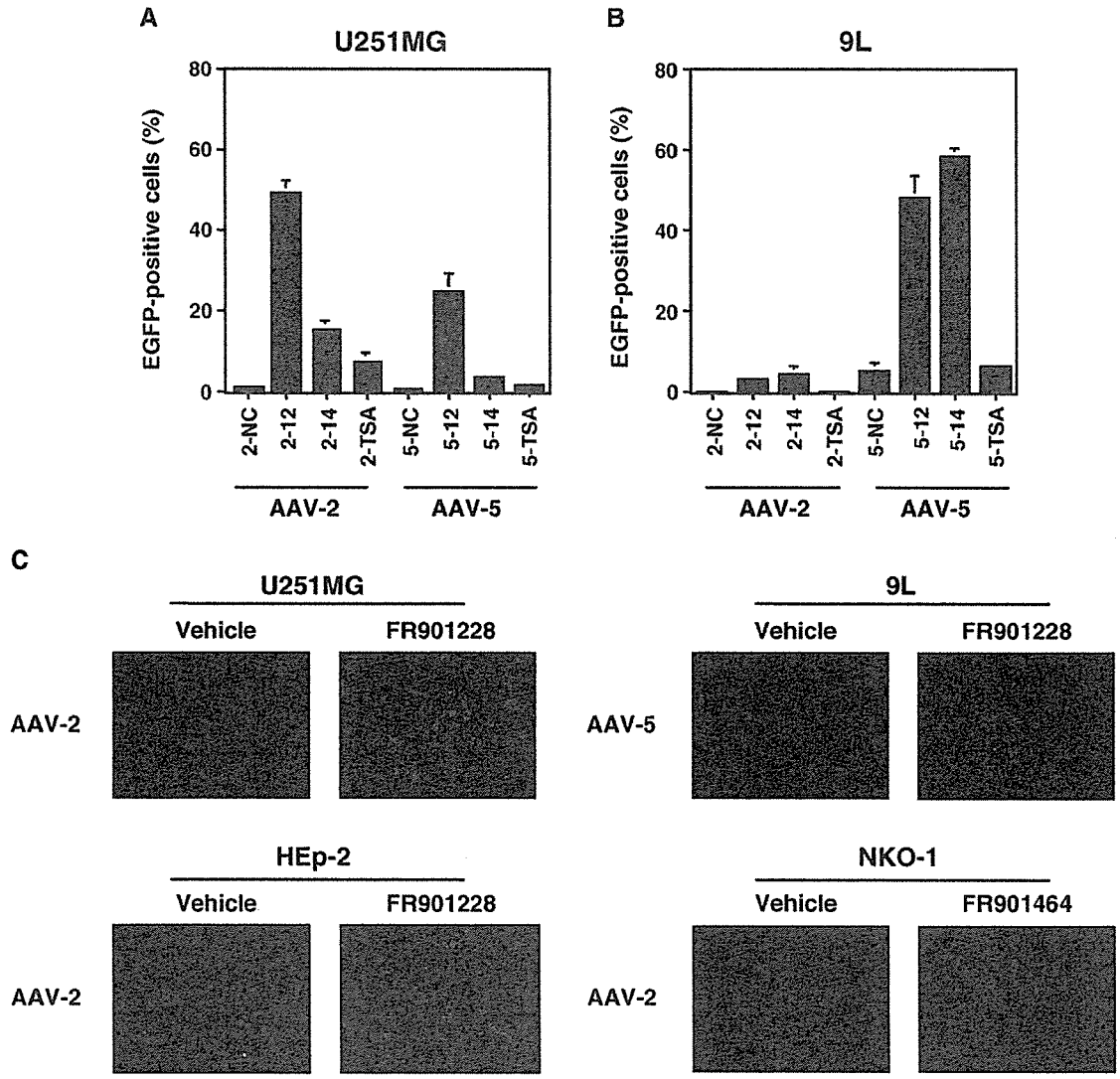

FIG. 3. (A, B) EGFP expression by AAV2EGFP and AAV5EGFP differs depending on the tumor cell being transduced. U251MG or 9L cells were infected with 1 × 10^4 genome copies/cell of AAV2EGFP (2) or AAV5EGFP (5) in the presence of vehicle (NC) or 1 ng/ml of various HDAC inhibitors, FR901228 (12), FR901464 (14), or TSA. The cells were analyzed by FACS 24 h after the infection. The data show the average percentages of EGFP-positive cells after three independent transductions + SD. (C) Representative data of the enhanced transgene expression by HDAC inhibitors in various cell lines infected with AAV vectors. Twenty-four hours after the AAV2EGFP or AAV5EGFP infection at 1 × 10^4 genome copies/cell with 1 ng/ml of the FR901228 or FR901464, cells were examined under the fluorescence microscope.

doi:10.1016/j.ymthe.2005.11.010

increased mRNA levels of fibroblast growth factor receptor 1 (FGF-R1) and platelet-derived growth factor receptor (PDGF-R), although the augmentation was not enough to explain the drastic increase of the expression (Table 1).

Transduction of Tumor Cells with AAV Vectors Derived from Distinct Serotypes

Type 2 and type 5 rAAV differed from each other in the efficiency of their transduction of U251MG and the 9L glioma cells. Although FR901228 and other HDAC inhibitors (FR901464 or trichostatin A (TSA)) remarkably enhanced the transduction of both rAAVs in general, AAV2EGFP-mediated transduction of U251MG cells was more efficient than AAV5EGFP-mediated transduction while AAV5EGFP-mediated transduction of 9L cells was better than AAV2EGFP-mediated transduction (Figs. 3A and 3B). FR901228 and FR901464 also had promoting effects on AAV2EGFP- and AAV5EGFP-mediated transduction of the head and neck cancer cell lines HEp-2 and NKO-1 (Fig. 3C).

Chromatin Modification with FR901228

We characterized chromatin composition of the episomal AAV vector genome by using the chromatin immunoprecipitation (ChIP) assay. ChIP is a technique to test for the presence of certain DNA-binding proteins that might modulate chromatin structure and/or transcriptional characteristics of the specific region of DNA with which they are associated. We made use of polyclonal antibodies generated against histone H3 as well as acetylated histone H3, which have been linked to chromatin modification and regulation of transcription. The primers for the CMV promoter region in the AAV vector genome gave a higher level of PCR product when used on templates from FR901228-treated cells compared to those from cells without FR901228 treatment. Higher levels of acetylated histone H3 were found on the CMV promoter region of the AAV vector versus the GAPDH promoter region of the cellular DNA (Table 2A). In contrast, enrichment of acetylated histone H3-associated DNA was not significant on plasmid vector genome irrespective of the presence of the ITR (Table 2B).

FR901228-Assisted Enhancement of Tumor Transduction *in Vivo*

In the analysis using optical bioluminescence imaging of the subcutaneous tumors, we confirmed drastic enhancement of the luciferase gene expression *in vivo* (Fig. 4A). The signal intensity in animals treated with FR901228 (n = 5, [1.5 ± 0.9] × 10^6 photons/s/cm^2/sr) was 37.4-fold higher than in control animals (n = 3, [4.0 ± 2.4] × 10^4 photons/s/cm^2/sr). A subcutaneous

TABLE 2: PCR amplification of immunoprecipitated DNA

(A) Chromatin composition of episomal AAV vector genome was characterized by using the chromatin immunoprecipitation assay

Ab of interest	FR901228	$2^{\text{correctedΔCt (GAPDHprom − CMVprom)}}$	
Rabbit IgG	−	<0.001	
Rabbit IgG	+	<0.001	
Anti-histone H3	−	1.0 ± 1.8	
Anti-histone H3	+	7.3 ± 1.4	
Anti-acetyl histone H3	−	1.0 ± 0.4	< 0.0001
Anti-acetyl histone H3	+	22.0 ± 0.8	

(B) Cells were transfected with a plasmid harboring the EGFP expression cassette under the CMV promoter (pEGFP) or a plasmid carrying an identical EGFP expression cassette flanked by ITR regions (pITR-EGFP)

Plasmid	Ab of interest	FR901228	$2^{\text{correctedΔCt (GAPDHprom − CMVprom)}}$
pEGFP	Rabbit IgG	−	<0.001
	Rabbit IgG	+	<0.001
	Anti-acetyl histone H3	−	1.0
	Anti-acetyl histone H3	+	1.3
pITR-EGFP	Rabbit IgG	−	<0.001
	Rabbit IgG	+	<0.001
	Anti-acetyl histone H3	−	1.0
	Anti-acetyl histone H3	+	1.2

U251MG cells were transduced with AAV vector at 1 × 10^4 genome copies/cell in the presence or absence of 1 ng/ml FR901228. Twenty-four hours after the transduction, chromatin proteins of interest were cross-linked to DNA by formaldehyde. Shared DNA was immunoprecipitated with histone H3 antibody or acetylated histone H3 antibody to enrich for the CMV promoter region or GAPDH promoter region. Relative differences in the levels of immunoprecipitated DNA, which are reflective of the levels of the chromatin protein of interest occupying a particular island, between different promoter regions and cell treatment with FR901228 were quantified by quantitative PCR.

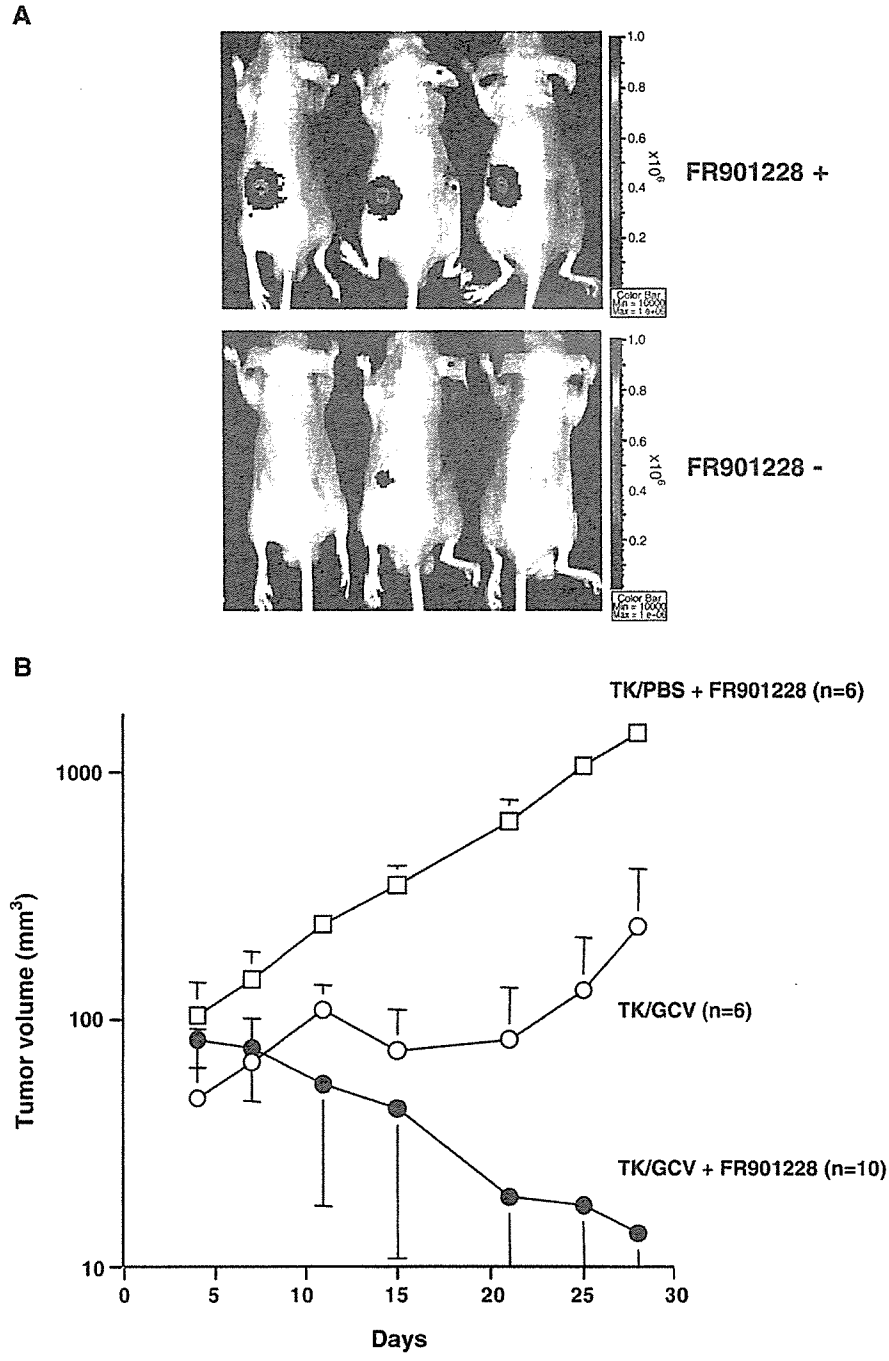

FIG. 4. (A) FR901228-assisted enhancement of tumor transduction *in vivo*. U251MG cells were mixed with PBS (FR901228–, $n = 3$) or transduced with a recombinant AAV2 expressing luciferase (AAV2Luc) at 1×10^4 genome copies/cell for 1 h (FR901228+, $n = 5$), and then 3×10^6 of the transduced cells in 100 μl PBS were inoculated subcutaneously into the BALB/c mice along with the intraperitoneal injection of FR901228 at 1 mg/kg. Twenty-four hours after administration of the FR901228, optical bioluminescence imaging was performed using the CCD camera. (B) The effects of FR901228 on the rAAV-mediated transduction for 9L tumor elimination *in vivo*. Cells were transduced with AAV5TK at 1×10^4 genome copies/cell for 1 h, and then 3×10^6 of the transduced cells in 100 μl PBS containing 25% (v/v) basement membrane matrix were inoculated subcutaneously into the BALB/c mice. The tumor-bearing animals received intraperitoneal injection of FR901228 at 3 mg/kg (group 1, $n = 6$; group 3, $n = 10$) or PBS (group 2, $n = 6$). The animals were also exposed to ganciclovir (GCV) at 100 mg/kg per day (groups 2 and 3) or PBS (group 1) for 14 consecutive days by intraperitoneal placement of the miniosmotic pumps.

tumor model with athymic nude mice demonstrated that the combination of AAV-mediated transduction for HSV-*tk*/GCV therapy and FR901228 treatment ($n = 10$) resulted in statistically significant reduction of tumor growth relative to HSV-*tk*/GCV therapy without FR901228 treatment (unpaired t test, $P < 0.05$, $n = 6$; Fig. 4B). When the tumor-bearing animals were treated with GCV and FR901228, 8 of 10 tumors were eliminated at 4 weeks after transduction.

Discussion

HDAC inhibitors significantly improved the expression of the transgene in cancer cells. The enhancement of the coreceptor level was modest and copy number of the

doi:10.1016/j.ymthe.2005.11.010

rAAV in the transduced cells was also modestly affected by the FR901228 treatment. Furthermore, association of the acetylated histone H3 in the episomal AAV vector genome was demonstrated by using the chromatin immunoprecipitation assay. In the analysis with the subcutaneous tumor models, strong enhancement of the transgene expression as well as therapeutic effect was confirmed *in vivo*.

Treatment with an HDAC inhibitor is known to cause the recovery of the gene expression of a rAAV vector genome that has been integrated and silenced after long-term selection [8]. However, rAAV occurs mostly as extrachromosomal genomes rather than as integrated genomes, and these extrachromosomal forms are the primary source of rAAV-mediated gene expression early after transduction [9]. There has been no direct investigation of the effects of HDAC inhibitors on the rAAV-mediated transient gene expression. We examined whether the HDAC inhibitor could contribute to the enhanced transcription before integration occurs.

FR901228 treatment significantly improved the transient expression of the transgene in four cancer cell lines. The FR901228 treatment improved the rAAV-mediated gene transfer in a dose-dependent manner, and the highest enhancement was observed in the U251MG cells with AAV2EGFP. In the U251MG cells, the cell surface levels of alpha v integrin, FGF-R1, and PDGF-R were only modestly enhanced by the presence of FR901228. These observations contrast with a previous report that suggested that FR901228 enhanced adenovirus transduction by increasing CAR and v integrin RNA levels, thereby enhancing viral entry [7]. However, their study did not demonstrate that these increased RNA levels were associated with increased protein levels or kinetics. In our study, a kinetic analysis of the effect on the FR901228-assisted AAV-mediated transduction of U251MG cells showed that the transduction efficiency peaked when cells were treated with FR901228 at the time of transduction. This is in sharp contrast to the case of the effect of FR901228 on the enhanced adenovirus-mediated transduction. Since enhanced viral entry into the cell is a primary function of FR901228 regarding improved adenovirus transduction, transduction efficiency of the adenovirus was preferentially enhanced when the cells were pretreated with FR901228 before transduction [10].

Interestingly, we observed that type 2 and type 5 rAAV differed from each other in the efficiency of their transduction of the U251MG and 9L cells. The differences in the transduction efficiency of the AAV vectors derived from distinct serotypes may be due to the fact that each AAV serotype recognizes a different receptor and that different cell types may express different levels of these receptors. Type 2 AAV uses the cell surface heparan sulfate proteoglycan (HSPG) as a receptor [11]. However, cell surface expression of HSPG alone is insufficient for type 2 AAV infection and FGF-R1 is also required as a coreceptor for successful viral entry into the host cell [12]. Type 5 AAV transduction requires 2,3-linked sialic acid [13] as well as PDGF-R [14] for efficient binding and transduction. These observations indicate that optimized expression of a transgene borne by rAAV will require the careful selection of the appropriate vector serotype with respect to the target cell.

Our data also suggest that the use of FR901228 in combination with AAV vector infection may improve viral entry into the cells, but also requires additional mechanisms to benefit the target cells for the efficient transduction. Association of the acetylated histone H3 in the episomal AAV vector genome was characterized by using the chromatin immunoprecipitation assay. Characterization of the chromatin modification in the rAAV genome with FR901228 suggested that improved expression of the transgene depends on the chromatin state of the AAV genome in the infected cells rather than viral entry. These results suggest that the superior transduction induced by HDAC inhibitor treatment is actually due to an enhancement of transgene expression associated with chromatin modification rather than to increased viral entry. Thus, epigenetic regulatory mechanisms may be involved in the HDAC inhibitor-mediated improvement of the transduction of cancer cells with rAAV. The rAAV concatemer may need to be present in a histone-associated chromatin form in the cells before efficient transgene expression can occur.

Our study suggests that the improved rAAV-mediated transduction induced by HDAC inhibitor was due to an enhancement of transgene expression rather than increased viral entry. This phenomenon may be related to the proposed histone-associated chromatin form of the rAAV concatemer in transduced cells. The depsipeptide fermentation product FR901228 is currently being tested in clinical trials as an anti-cancer drug. Therefore, to utilize such a compound to assist rAAV-mediated cancer gene therapy is theoretically and practically reasonable. The use of HDAC inhibitors may enhance the utility of rAAV-mediated transduction strategies for future clinical investigation.

Materials and Methods

Recombinant AAV production. The EGFP expression cassette driven by the CMV promoter was ligated into pAAVLacZ [15] and pAAV5-RNL [16] to form the proviral plasmids pAAV2EGFP and pAAV5EGFP. rAAV types 2 and 5 that express the EGFP gene (AAV2EGFP and AAV5EGFP) were generated using the proviral plasmids. The luciferase expression cassette driven by the CMV promoter in pLNCL [17] was cloned into pAAVLacZ to create pAAV2Luc. A rAAV type 2 that expresses the luciferase gene (AAV2Luc) was generated using pAAV2Luc. Likewise, the HSV-*tk* cDNA contained in the pAVS6TK [18] was subcloned into pAAV5-RNL to create pAAV5TK. A rAAV type 5 that expresses the HSV-*tk* gene driven by the CMV promoter (AAV5TK) was generated using pAAV5TK. Transfection of 293 cells with the proviral plasmid, AAV helper plasmid pAAV2H [15] or pAAV5H [16], and adenoviral helper plasmid pAdeno was performed according to the previously described protocol [19] associated with an

active gassing [20]. The physical titer of the viral stock was determined by dot-blot hybridization with plasmid standards.

HDAC inhibitors. The HDAC inhibitor FR901228 (obtained from Fujisawa Pharmaceutical Co., Ltd.) is a depsipeptide fermentation product from *Chromobacterium violaceum* [21]. FR901228 strongly inhibits the proliferation of tumor cells by arresting cell cycle transition and is now being tested in clinical trials [22]. FR901464 (obtained from Fujisawa Pharmaceutical Co., Ltd.) and TSA (Sigma–Aldrich Corp., St. Louis, MO, USA) are also prepared as HDAC inhibitors [21].

Cells and culture. The malignant human glioma cell line U251MG, the malignant rat glioma cell line 9L, the laryngeal epidermoid carcinoma cell line HEp-2, and the human maxillary sinus cancer cell line NKO-1 were used in this study. Cells were cultured in Dulbecco's modified Eagle medium (D-MEM) supplemented with 10% fetal bovine serum (FBS), 100 units/ml penicillin, and 100 μg/ml streptomycin at 37°C, 5% CO_2. Human embryonic kidney 293 cells were cultured with D-MEM:F12 (1:1 mixture) supplemented with 10% FBS, 100 units/ml penicillin, and 100 μg/ml streptomycin at 37°C, 5% CO_2. Luciferase assay was performed on the luminometer (Fluoroskan Ascent FL, Thermo Labsystems, Beverly, MA, USA) using the Bright-Glo Reagent kit (Promega, Madison, WI, USA).

FACS analysis. Approximately 5×10^4 cells were analyzed on the FACScan (Becton–Dickinson, San Jose, CA, USA) with CellQuest software (Becton–Dickinson). Cells were incubated with a PE-labeled monoclonal antibody (13C2) specific for human integrin v chain (CD51; Cymbus Biotechnology Ltd., Chandlers Ford, UK) for 30 min on ice. The 7-aminoactinomycin-D (Via-Probe; Pharmingen, San Diego, CA, USA)-negative cell fraction, which contains the viable cells, was used to detect EGFP- and/or PE-positive cells.

Western blot analysis. Detection of histone acetylation by FR901228 in U251MG cells was performed as described [7]. Western blot analysis of the cells incubated in the presence or absence of FR901228 for 24 h was performed using either a rabbit polyclonal antibody against histone H3 or one against acetylated histone H3 (Upstate Biotechnology, Lake Placid, NY, USA) diluted 1:2000 in 5% milk. The probed membrane was incubated with an anti-rabbit immunoglobulin horseradish peroxidase-linked antibody and developed by ECL Western blotting detection reagents (Amersham Pharmacia Biotech, Piscataway, NJ, USA).

Determination of transgene copy number. Tumor cells were infected with 1×10^4 genome copies/cell of rAAV in the presence of FR901228. The high-molecular-weight DNA was extracted from the cells (DNA Extraction Kit; Qiagen, Inc., Hilden, Germany) 0, 2, 4, 12, and 24 h later. The copy numbers were determined by quantitative PCR analysis of 100 ng of the DNA by using an ABI Prism 7700 sequence detection system (Applied Biosystems, Foster City, CA, USA) as described in the supplementary information.

mRNA analysis of coreceptors for the AAV. U251MG cells were incubated with recombinant AAV either alone (1×10^4 genome copies/cell) or together with FR901228 (0.3 or 3 ng/ml) for 24 h. mRNA was isolated from the cell culture using an RNeasy mini kit (Qiagen) and reverse-transcribed into a single-stranded cDNA using the SuperScript Preamplification System (Invitrogen, Carlsbad, CA, USA). FGF-R1 or PDGF-R mRNA was quantitated by real-time PCR as described in the supplementary information.

PCR analysis of immunoprecipitated DNA. Chromatin immunoprecipitation was performed following the Upstate Biotechnology ChIP kit protocol. U251MG cells were transduced with AAV vector at 1×10^4 genome copies/cell, pCMV-EGFP, or pAAV2EGFP in the presence or absence of the 1 ng/ml FR901228. Twenty-four hours after the transduction, chromatin proteins of interest were cross-linked to DNA. After preclearing, isotype-antibody control or anti-acetylated histone H3 or anti-histone H3 antibody (Upstate Biotechnology) was added to the sonicated chromatin solution and incubated overnight at 4°C with agitation. Resulting immune complexes were collected by the salmon sperm DNA–protein A agarose slurry. The eluted samples were treated with proteinase K and purified by phenol/chloroform extraction. Precipitated DNAs were analyzed for the vector-derived promoter by quantitative PCR with an ABI Prism 7700 sequence detection system as described in the supplementary information.

In vivo analysis of enhanced transgene expression. U251MG cells were treated with PBS ($n = 3$) or transduced with a recombinant AAV2 expressing luciferase (AAV2Luc) at 1×10^4 genome copies/cell for 1 h ($n = 5$), and then 3×10^6 of the transduced cells in 100 μl PBS containing 25% (v/v) basement membrane matrix (Matrigel; BD Biosciences, Franklin Lakes, NJ, USA) were inoculated subcutaneously into male BALB/c *nu/nu* mice (Clea Japan, Tokyo, Japan) along with intraperitoneal injection of FR901228 at 1 mg/kg or the same volume of vehicle. Twenty-four hours after the administration of FR901228, optical bioluminescence imaging was performed using the CCD camera (Xenogen Corp., Alameda, CA, USA). After intraperitoneal injection of reporter substrate D-luciferin (375 mg/kg body wt), mice were imaged for scans.

To analyze the effect of FR901228 on the enhanced tumor elimination *in vivo*, 9L tumor cells were transduced with an AAV5TK at 1×10^4 genome copies/cell for 1 h, and then 3×10^6 of the transduced cells in 100 μl PBS containing 25% (v/v) Matrigel were inoculated subcutaneously into BALB/c mice. The tumor-bearing animals received an intraperitoneal injection of FR901228 at 3 mg/kg (group 1, $n = 6$; group 3, $n = 10$) or PBS (group 2, $n = 6$). The animals were also exposed to ganciclovir at 100 mg/kg per day (groups 2 and 3) or PBS (group 1) for 14 consecutive days by intraperitoneal placement of the miniosmotic pumps (Alzet, Palo Alto, CA, USA) according to the manufacturer's instructions. Tumor growth was monitored two to three times a week by measuring two perpendicular tumor diameters using calipers and the volumes were calculated as $a \times b^2 \times 0.5$, where a is the length and b is the width of the tumor in millimeters. Animals with tumors larger than 2 cm in diameter were euthanized.

ACKNOWLEDGMENTS

FR901228 and FR901464 were kindly provided by Fujisawa Pharmaceutical Co., Ltd. We thank Avigen, Inc. (Alameda, CA, USA) for providing pAAV2H (identical to pHLP19) and pAdeno. We are also indebted to Dr. John A. Chiorini for providing pAAV5H (identical to 5RepCapB) and pAAV5RNL. We also thank Ms. Miyoko Mitsu for her encouragement and support. This study was supported in part by (1) grants from the Ministry of Health, Labor, and Welfare of Japan, (2) Grants-in-Aid for Scientific Research, (3) a grant from the 21st Century COE Program, and (4) the "High-Tech Research Center" Project for Private Universities, matching fund subsidy, from the Ministry of Education, Culture, Sports, Science, and Technology of Japan.

RECEIVED FOR PUBLICATION SEPTEMBER 20, 2005; REVISED OCTOBER 25, 2005; ACCEPTED NOVEMBER 19, 2005.

APPENDIX A. SUPPLEMENTARY DATA

Supplementary data associated with this article can be found in the online version at doi:10.1016/j.ymthe.2005.11.010.

REFERENCES

1. Carter, B. J. (2004). Adeno-associated virus and the development of adeno-associated virus vectors: a historical perspective. *Mol. Ther.* **10:** 981–989.
2. Okada, T., *et al.* (2002). Adeno-associated virus vectors for gene transfer to the brain. *Methods* **28:** 237–247.
3. Zaiss, A. K., Liu, Q., Bowen, G. P., Wong, N. C., Bartlett, J. S., and Muruve, D. A. (2002). Differential activation of innate immune responses by adenovirus and adeno-associated virus vectors. *J. Virol.* **76:** 4580–4590.
4. Kanazawa, T., *et al.* (2001). Gamma-rays enhance rAAV-mediated transgene expression and cytocidal effect of AAV-HSVtk/ganciclovir on cancer cells. *Cancer Gene Ther.* **8:** 99–106.
5. Kanazawa, T., *et al.* (2003). Suicide gene therapy using AAV-HSVtk/ganciclovir in

doi:10.1016/j.ymthe.2005.11.010

combination with irradiation results in regression of human head and neck cancer xenografts in nude mice. *Gene Ther.* **10:** 51–58.
6. Kanazawa, T., *et al.* (2004). Topoisomerase inhibitors enhance the cytocidal effect of AAV-HSVtk/ganciclovir on head and neck cancer cells. *Int. J. Oncol.* **25:** 729–735.
7. Kitazono, M., Goldsmith, M. E., Aikou, T., Bates, S., and Fojo, T. (2001). Enhanced adenovirus transgene expression in malignant cells treated with the histone deacetylase inhibitor FR901228. *Cancer Res.* **61:** 6328–6330.
8. Chen, W. Y., Bailey, E. C., McCune, S. L., Dong, J. Y., and Townes, T. M. (1997). Reactivation of silenced, virally transduced genes by inhibitors of histone deacetylase. *Proc. Natl. Acad. Sci. USA* **94:** 5798–5803.
9. Nakai, H., Yant, S. R., Storm, T. A., Fuess, S., Meuse, L., and Kay, M. A. (2001). Extrachromosomal recombinant adeno-associated virus vector genomes are primarily responsible for stable liver transduction in vivo. *J. Virol.* **75:** 6969–6976.
10. Vanoosten, R. L., Moore, J. M., Ludwig, A. T., and Griffith, T. S. (2005). Depsipeptide (FR901228) enhances the cytotoxic activity of TRAIL by redistributing TRAIL receptor to membrane lipid rafts. *Mol. Ther.* **11:** 542–552.
11. Summerford, C., and Samulski, R. J. (1998). Membrane-associated heparan sulfate proteoglycan is a receptor for adeno-associated virus type 2 virions. *J. Virol.* **72:** 1438–1445.
12. Qing, K., Mah, C., Hansen, J., Zhou, S., Dwarki, V., and Srivastava, A. (1999). Human fibroblast growth factor receptor 1 is a co-receptor for infection by adeno-associated virus 2. *Nat. Med.* **5:** 71–77.
13. Walters, R. W., *et al.* (2001). Binding of adeno-associated virus type 5 to 2,3-linked sialic acid is required for gene transfer. *J. Biol. Chem.* **276:** 20610–20616.
14. Di Pasquale, G., *et al.* (2003). Identification of PDGFR as a receptor for AAV-5 transduction. *Nat. Med.* **9:** 1306–1312.
15. Okada, T., *et al.* (2001). Development and characterization of an antisense-mediated prepackaging cell line for adeno-associated virus vector production. *Biochem. Biophys. Res. Commun.* **288:** 62–68.
16. Chiorini, J. A., Kim, F., Yang, L., and Kotin, R. M. (1999). Cloning and characterization of adeno-associated virus type 5. *J. Virol.* **73:** 1309–1319.
17. Okada, T., *et al.* (1997). Inhibition of gene expression from the human c-erbB gene promoter by a retroviral vector expressing anti-gene RNA. *Biochem. Biophys. Res. Commun.* **240:** 203–207.
18. Okada, T., *et al.* (2001). AV.TK-mediated killing of subcutaneous tumors in situ results in effective immunization against established secondary intracranial tumor deposits. *Gene Ther.* **8:** 1315–1322.
19. Okada, T., *et al.* (2002). Adeno-associated viral vector-mediated gene therapy of ischemia-induced neuronal death. *Methods Enzymol.* **346:** 378–393.
20. Okada, T., *et al.* (2005). Large-scale production of recombinant viruses using a large culture vessel with active gassing. *Hum. Gene Ther.* **16:** 1212–1218.
21. Nakajima, H., Kim, Y. B., Terano, H., Yoshida, M., and Horinouchi, S. (1998). FR901228, a potent antitumor antibiotic, is a novel histone deacetylase inhibitor. *Exp. Cell Res.* **241:** 126–133.
22. Sandor, V., *et al.* (2002). Phase I trial of the histone deacetylase inhibitor, depsipeptide (FR901228, NSC 630176), in patients with refractory neoplasms. *Clin. Cancer Res.* **8:** 718–728.

Oncogene (2006) 25, 512–524

www.nature.com/onc

ORIGINAL ARTICLE

Histone deacetylase inhibitor FK228 suppresses the Ras–MAP kinase signaling pathway by upregulating Rap1 and induces apoptosis in malignant melanoma

Y Kobayashi[1,2], M Ohtsuki[2], T Murakami[2,3], T Kobayashi[1,4], K Sutheesophon[1], H Kitayama[5], Y Kano[6], E Kusano[4], H Nakagawa[7] and Y Furukawa[1]

[1]Division of Stem Cell Regulation, Jichi Medical School, Yakushiji, Minamikawachi-machi, Tochigi, Japan; [2]Department of Dermatology, Jichi Medical School, Yakushiji, Minamikawachi-machi, Tochigi, Japan; [3]Divison of Organ Transplantation, Jichi Medical School, Yakushiji, Minamikawachi-machi, Tochigi, Japan; [4]Department of Nephrology, Jichi Medical School, Yakushiji, Minamikawachi-machi, Tochigi, Japan; [5]Department of Molecular Oncology, Kyoto University Graduate School of Medicine, Yoshida-Konoe-cho, Sakyo-ku, Kyoto, Japan; [6]Division of Medical Oncology, Tochigi Cancer Center, Yonan, Utsunomiya, Tochigi, Japan and [7]Department of Dermatology, Jikei University School of Medicine, Nishi-Shinbashi, Minato-ku, Tokyo, Japan

Histone deacetylase (HDAC) inhibitors are expected to be effective for refractory cancer because their mechanism of action differs from that of conventional antineoplastic agents. In this study, we examined the effect of the HDAC inhibitor FK228 on malignant melanoma, as well as its molecular mechanisms. FK228 was highly effective against melanoma compared with other commonly used drugs. By comparing the gene expression profiles of melanoma cells and normal melanocytes, we defined a subset of genes specifically upregulated in melanoma cells by FK228, which included Rap1, a small GTP-binding protein of the Ras family. The expression of Rap1 mRNA and protein increased in FK228-treated melanoma cells in both a dose- and a time-dependent manner. A decrease in the phosphorylation of c-Raf, MEK1/2, and ERK1/2 was accompanied by an increase in Rap1 expression in both FK228-treated and Rap1-overexpressing cells. Inhibition of Rap1 upregulation by small interfering RNA (siRNA) abrogated the induction of apoptosis and suppression of ERK1/2 phosphorylation in FK228-treated melanoma cells. These results indicate that the cytotoxic effects of FK228 are mediated via the upregulation of Rap1. Furthermore, we found that Rap1 was overexpressed and formed a complex with B-Raf in melanoma cell lines with a V599E mutation of B-Raf. The siRNA-mediated abrogation of Rap1 overexpression increased the viability of these cells, suggesting that Rap1 is also an endogenous regulator of Ras–MAP kinase signaling in melanomas.
Oncogene (2006) **25,** 512–524. doi:10.1038/sj.onc.1209072; published online 26 September 2005

Keywords: melanoma; histone deacetylase inhibitor; Raf; MAP kinase; Rap1; apoptosis

Correspondence: Dr Y Furukawa, Division of Stem Cell Regulation, Center for Molecular Medicine, Jichi Medical School, 3311-1 Yakushiji, Minamikawachi-machi, Tochigi 329-0498, Japan.
E-mail: furuyu@jichi.ac.jp
Received 4 March 2005; revised 26 July 2005; accepted 29 July 2005; published online 26 September 2005

Introduction

Malignant melanoma is an extremely aggressive neoplasm with high mortality. The survival rate is 12% over 5 years and less than 1% over 10 years in patients with stage IV disease (Francken *et al.*, 2004). There are two major reasons for this poor prognosis: first, most patients have advanced disease, including distant metastasis, upon initial presentation. Second, melanoma cells are highly resistant to conventional chemotherapy (Soengas and Lowe, 2003). At present, the most effective regimen for malignant melanoma is DAV-F, which is composed of dacarbazine, adriamycin, vincristine, and interferon-β. In spite of the increase in the remission rate from 15% in patients treated with dacarbazine alone to 30%, this combination has failed to prolong overall survival of patients with advanced melanoma (Helmbach *et al.*, 2001). Therefore, a novel treatment strategy based on a better understanding of the molecular basis of this disease is in high demand.

Aberrant transcriptional repression of genes regulating cell growth and differentiation is a hallmark of cancer (Herman and Baylin, 2003). Recently, evidence has accumulated suggesting that the altered activation of histone deacetylases (HDACs) underlies the transcriptional repression in malignancies (Marks *et al.*, 2001). This is best illustrated in the case of leukemogenesis. In leukemogenesis, various leukemic fusion proteins, generated by reciprocal chromosomal translocations, form a complex with HDACs with higher affinity than that of their normal counterparts; this complex in turn aberrantly represses the genes required for cell differentiation and growth control, leading to the transformation of primitive hematopoietic cells (Hong *et al.*, 1997; Lin *et al.*, 1998). In solid tumors, including colon cancer and malignant melanoma, which do not possess fusion proteins, the overexpression of HDACs is believed to contribute to oncogenesis in a similar manner (Zhu *et al.*, 2004; Kobayashi *et al.*, manuscript in preparation).

Given the role of HDACs in oncogenesis, the use of small compounds that inhibit HDAC activity, collectively referred to as HDAC inhibitors, is expected to become a novel strategy for the treatment of cancer called 'transcription therapy' (Somech *et al.*, 2004). HDAC inhibitors are able to restore the expression of genes that are aberrantly suppressed in cancer cells, which may result in cell cycle arrest, differentiation, and apoptosis (Kim *et al.*, 2003). Because the principle of action differs from that of other anticancer drugs, HDAC inhibitors may be effective for malignancies that are otherwise resistant to conventional chemotherapy. Indeed, HDAC inhibitors have been shown to exert cytotoxic effects on various tumor cell lines and primary cancer cells *in vitro* (Hoshikawa *et al.*, 1994). Furthermore, Zhu *et al.* (2004) reported that HDAC inhibitors were capable of reducing tumor formation on intestinal tracts of mice bearing mutations in the adenomatous polyposis coli (APC) tumor suppressor gene. Currently, phase I and II clinical trials are ongoing for four different types of HDAC inhibitors, namely sodium phenylbutyrate, FK228 (a bacterial depsipeptide, formerly FR901228), suberoylanilide hydroxamic acid (SAHA), and MS-275, in hematologic malignancies and various solid tumors (Gore *et al.*, 2002; Sandor *et al.*, 2002).

FK228 is one of the most promising HDAC inhibitors for the treatment of malignant melanoma because of its potent antitumor activity. This drug was isolated from *Chromobacterium violaceum* No. 968 as a compound that reversed the malignant phenotypes of H-ras-transformed fibroblasts by blocking the $p21^{ras}$-mediated signal transduction pathways (Ueda *et al.*, 1994). In independent studies, FK228 was identified as a microbial metabolite that induces transcriptional activation of the SV40 promoter via inhibition of intracellular HDAC activities (Nakajima *et al.*, 1998; Furumai *et al.*, 2002). FK228 was reported to inhibit proliferation and induce apoptosis in primary and metastatic uveal melanoma cell lines *in vitro* (Klisovic *et al.*, 2003), and exhibited therapeutic effects on a diverse range of malignancies, including melanoma, in phase I and II clinical trials (Gore *et al.*, 2002; Sandor *et al.*, 2002). However, the safe and effective clinical application of this agent will require clarification of the molecular basis of its cytotoxic activity. In the present study, we investigated the cytotoxic effect of FK228 on malignant melanoma and its mechanism of action using six melanoma cell lines. We have found that (1) FK228 is more effective against malignant melanoma than other commonly used anticancer drugs, (2) the cytotoxic effects of FK228 are at least in part mediated by the upregulation of Rap1, a small GTP-binding protein of the Ras family, and (3) Rap1 is an intrinsic regulator of the Ras–Raf–MAP kinase signaling pathway in melanoma cells.

Results

FK228 is more effective for malignant melanoma than other commonly used anticancer drugs

We first evaluated the therapeutic efficacy of FK228 against malignant melanoma. For this purpose, we cultured the human melanoma cell line MM-LH with various concentrations of FK228 and other drugs commonly used for the treatment of melanoma, and determined the level of 5-bromo-2′-deoxyuridine (BrdU) incorporation after 48 h. As shown in Figure 1a, FK228 effectively inhibited the growth of MM-LH in a dose-dependent manner; BrdU incorporation decreased to less than 50% of that of the untreated control with 100 nM of the drug and to approximately 10% at a dose of 1 μM, which corresponds to the mean maximum plasma concentration ($C_{max.}$) determined in phase I clinical trials (Sandor *et al.*, 2002). In contrast, the other three drugs (adriamycin, vincristine, and interferon-β) failed to induce a decrease in BrdU incorporation at $C_{max.}$ (Figure 1a). The difference in the efficacy between FK228 and other drugs was statistically significant ($P<0.001$).

Next, we examined the cytotoxic effects of FK228 on normal human melanocytes. As shown in Figure 1b, FK228 was found to be less toxic to normal human epidermal melanocytes (NHEM) grown in the presence of melanocyte-growth medium than to three other melanoma cell lines MM-AN, MM-BP, and RPM-MC ($P<0.001$).

We further confirmed the antimelanoma effects of the drug *in vivo* using an animal model system. SCID mice carrying subcutaneous MM-LH xenografts were treated with intraperitoneal injection of FK228. As shown in Figure 1c, FK228 significantly retarded the growth of the xenografts compared with control (phosphate-buffered saline (PBS) alone) ($P=0.016$ at day 20) without obvious side effects. Taken together, these results strongly encourage the clinical application of FK228 for malignant melanoma.

DNA chip analysis has revealed candidate FK228 effector genes

Because the principal mechanism of action of HDAC inhibitors is the modulation of transcription, it is reasonable to screen for changes in gene expression as an initial step in exploring the mechanisms of the cytotoxic effects of FK228. To determine the optimal conditions for gene expression analysis, we first determined the time course of the effects of FK228 using the MM-LH cell line. Cell cycle analysis was serially performed with MM-LH cells cultured in the absence or presence of FK228 at a concentration of 100 nM, approximately the IC_{50} of this drug. FK228 induced both cell cycle arrest at the G1 phase and apoptosis, as judged by the appearance of the sub-G1 fraction (Figure 1d, upper panel), DNA fragmentation in the nuclei (Figure 1d, lower panel), and annexin V-positive cells (data not shown), after 24 h of culture. The time course of the response to the drug was almost identical to that of other melanoma cell lines (data not shown).

According to this result, we decided to perform a DNA chip analysis using RNA samples isolated at 6 h of culture, a time point at which the changes on the DNA histograms were minimal. The results of the analysis are summarized in Table 1: 20 genes showed more than a

fivefold increase in mRNA expression after FK228 treatment among 3893 human cancer-related and cytokine genes screened. The same analysis was performed using normal melanocytes in order to determine the subset of genes specifically upregulated in melanoma cells. We provisionally defined FK228 effector genes as

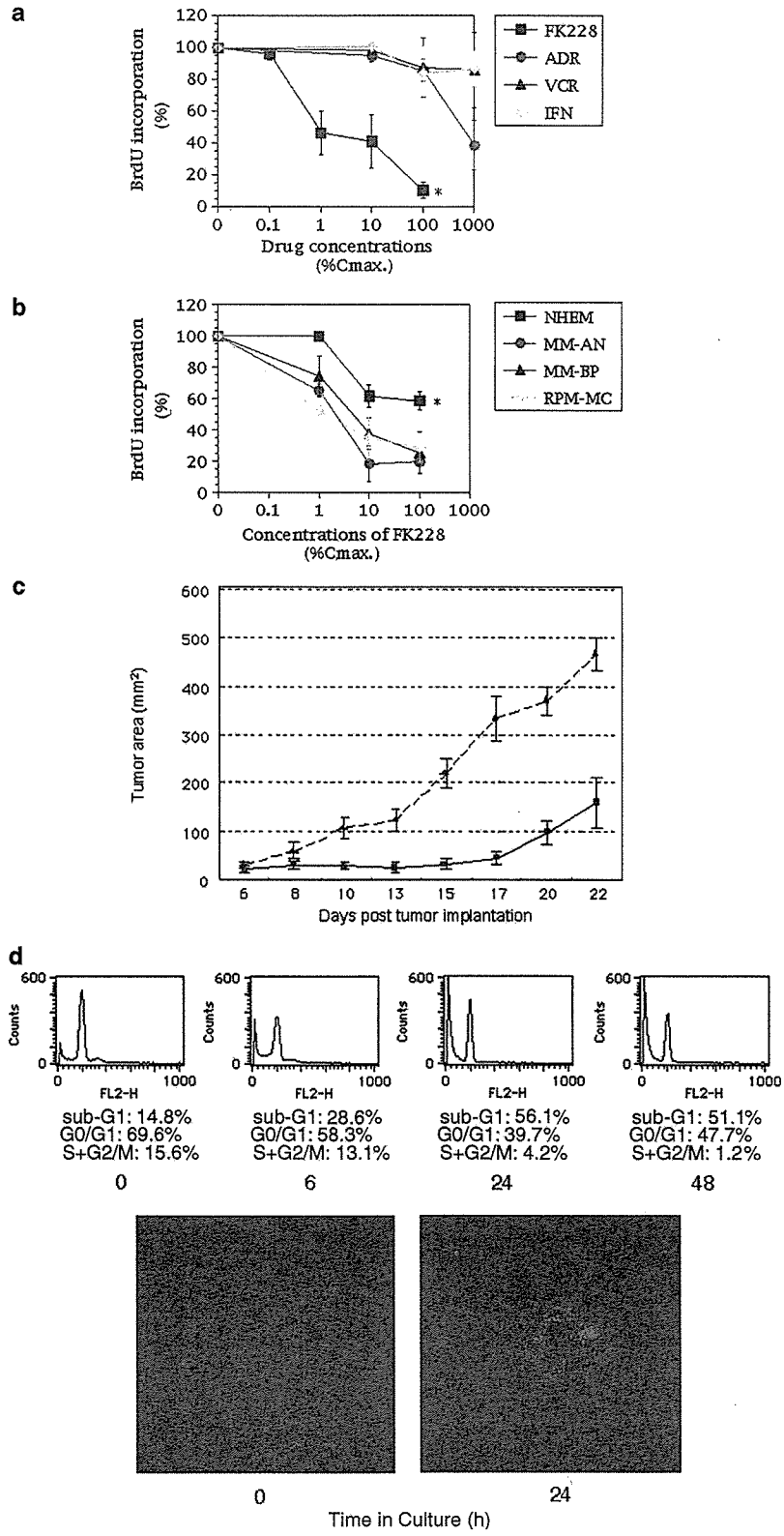

follows: genes upregulated more than fivefold in melanoma cells and less than twofold in normal melanocytes. Among 20 FK228-induced genes, seven genes fulfilled the criteria for FK228 effector genes: Silver-like (gp100/pMel17), TNF-α-induced protein 6, Rap1A, ADP-ribosylation factor 4, FLJ23028 (c-mer homolog), Coiled-coil forming protein 1, and TFIIB (Table 1). We chose Rap1 for further investigation of its involvement in the antimelanoma effects of FK228, because Rap1, a small GTP-binding protein of the Ras family, was originally isolated as Krev-1 by virtue of its ability to revert the malignant phenotype of activated Ras-transformed fibroblasts back to normal (Kitayama *et al.*, 1989), which is identical to the approach used for the initial discovery of FK228.

FK228 increases the expression of Rap1 and suppresses the activity of other components of the Ras–MAP kinase signaling pathway in melanoma cells

To confirm the upregulation of Rap1 by FK228, we carried out Northern blotting using MM-LH and RPMI-MC melanoma cell lines. Consistent with the results of the DNA chip analysis, the abundance of the Rap1 (Rap1A) transcript increased more than fivefold in FK228-treated cells, whereas no change was observed in untreated cells (Figure 2a, and data not shown). Importantly, the level of Rap1A mRNA remained below the detection limit in NHEM, even after treatment with FK228. We simultaneously examined the expression of Rap1B, a close relative of Rap1A/Krev-1 with a different chromosomal location (Bokoch,

Table 1 Genes whose expression was increased more than fivefold following FK228 treatment of melanoma cells[a]

Gene name[b]	*Accession number*	*Fold increase*[c]	*Increase in normal melanocytes*[d]
Interleukin-8	NM_000584	25.40 (94/3.7)	5.00 (74/14.8)
Fatty acid-binding protein 4	NM_001445	22.84 (1695/74.2)	122.54 (13968/114)
Silver-like	NM_006928	15.12 (270/17.85)	0.80 (48789/60986)
TNF-α-induced protein 6	NM_007115	12.55 (1066/84.9)	Not detected
Rap1A	BC034049	8.81 (690/78.3)	1.20 (32/26.7)
c-*fos*	NM_005252	8.21 (752/91.6)	5.71 (353/61.8)
SBB126	AK056390	7.49 (752/100.4)	2.76 (186/67.4)
ADP-ribosylation factor 4	NM_001661	7.23 (276/38.2)	1.58 (186/118)
FLJ23028	AK026681	6.23 (87/13.96)	0.88 (2/2.3)
Lipin1	D80010	5.76 (612/106.3)	2.23 (281/126)
FLJ22548	NM_022456	5.70 (439/77)	3.99 (289/72.4)
KIAA0870	AB020677	5.39 (123/22.8)	54.07 (260/4.80)
Coiled-coil forming protein 1	NM_014781	5.31 (1833/345.2)	1.96 (345/176)
KIAA0080	D38522	5.30 (1099/207.4)	9.95 (1359/136.6)
CDABP0105	AY007156	5.29 (270/51)	8.86 (207/23.4)
Nerve growth factor receptor	NM_002507	5.22 (152/29.1)	4.79 (150/31.3)
TFIIB	M76766	5.18 (799/154.2)	1.74 (603/346.6)
FEN1/Elo2	NM_022726	5.15 (164/31.8)	3.15 (73/23.2)
MHC class II peptide-related sequence A	NM_000247	5.12 (550/107.4)	4.62 (947/205)
Ephrin-B2	NM_004093	5.10 (44/8.63)	2.35 (76/32.3)

[a]Poly(A) RNAs were isolated from MM-LH cells treated with 100 nM FK228 for 6 h and from the untreated control, labeled with Cy5 and Cy3, respectively, and were hybridized to IntelliGene II human CHIP version 1.0 (Takara), which contains cDNA fragments of 3893 human cancer-related and cytokine genes. Precise information about this array is available at the company's website (http://www.takara.com). [b]FK228 effector genes are highlighted in bold (see text for definition). [c]Normalized expression values are shown in parentheses (treated/untreated). [d]The same experiments were carried out using normal human epidermal melanocytes.

Figure 1 Sensitivity of melanoma cells and normal melanocytes to FK228. (**a**) MM-LH cells were exposed to various concentrations of FK228, adriamycin (ADR), vincristine (VCR), and interferon-β (IFN-β) for 48 h, and cell growth was monitored by BrdU incorporation. Drug concentrations are expressed as the percentage of the mean maximum plasma concentration at the maximum tolerated dose (%$C_{max.}$). The $C_{max.}$ is 1 μM, 1 μg/ml, 100 nM, and 1000 U/ml for FK228, ADR, VCR, and IFN, respectively. BrdU incorporation is shown as the percentage of the value obtained with untreated cells. The results are the means$\pm$s.d. (bar) of three independent experiments. Statistical analysis was performed using the Student's *t*-test to compare the data from cells treated with FK228 and other drugs (an asterisk denotes $P<0.001$). (**b**) The same experiments were performed with NHEM and three different melanoma cell lines. Statistical analysis was carried out using the Student's *t*-test for comparative analysis of the data from NHEM and other cell lines (an asterisk denotes $P<0.001$). (**c**) MM-LH cells (1×10^7 cells/mouse) were injected subcutaneously into SCID mice. After tumors were palpable, animals were treated with either FK228 (0.5 mg/kg, intraperitoneally, every other day) or PBS. Serial measurement of tumor sizes in FK228- and PBS-treated mice was made. Slide line: FK228 treatment; dashed line: PBS treatment. Data represent the means$\pm$s.d. ($n=5$). Statistical analysis was carried out using the Mann–Whitney U test ($P=0.016$ at day 20). (**d**) MM-LH cells were seeded at 1×10^5 cells/ml and cultured in the presence of 100 nM FK228 for 48 h. Cells were harvested at the indicated time points, and subjected to cell cycle analysis (upper panel) and a TUNEL assay (lower panel). The size of the sub-G1, G0/G1, and S + G2/M fractions was calculated using the ModFitLT 2.0 program, and the results are shown below each DNA histogram. The data shown are representative of three independent experiments.

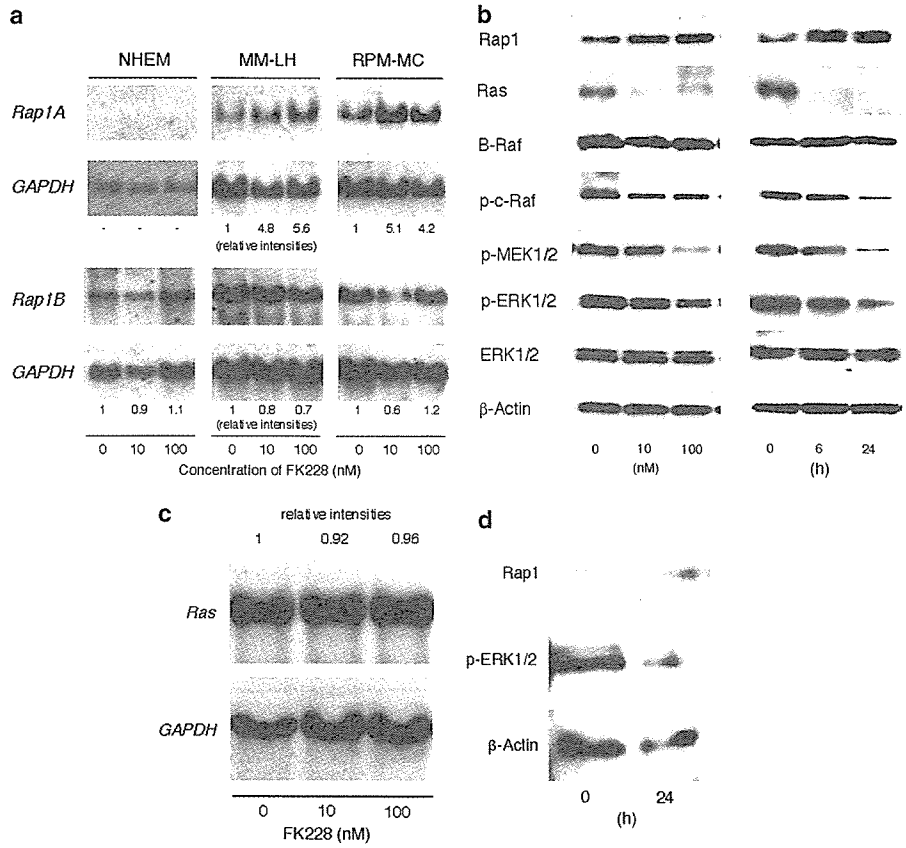

Figure 2 Expression of Rap1 and the components of the Ras–MAP kinase signaling pathway in FK228-treated melanoma cells and normal melanocytes. (**a**) Total cellular RNA was isolated from normal melanocytes (NHEM), and MM-LH and RPM-MC cell lines cultured with the indicated concentrations of FK 228 for 24 h, and was subjected to Northern blot analysis for Rap1A and Rap1B mRNA expression. The membrane filters were rehybridized with glyceroaldehyde-3-phosphate dehydrogenase (GAPDH) cDNA to serve as a loading control. The relative intensities of the signals were calculated as the fold increase from the value obtained in untreated cells (FK228 0 nM) after being normalized to the signal intensities of the corresponding GAPDH transcripts. (**b**) Whole-cell lysates were prepared from MM-LH cells cultured with various concentrations of FK228 for 24 h or with 100 nM FK228 for the indicated periods of time. The expression of Rap1 and the indicated components of the Ras–Raf–ERK signaling pathway was examined by immunoblotting using specific antibodies (p- indicates phosphorylated species). The membrane filters were reprobed with β-actin antibody in order to verify the equal loading of samples. (**c**) Ras mRNA expression was examined by Northern blotting in FK228-treated MM-LH cells. Relative signal intensities are shown on top. (**d**) Normal human melanocytes were cultured in the growth medium in the presence of 100 nM FK228 for 24 h, and subjected to immunoblotting for Rap1 and phosphorylated ERK1/2.

1993; Noda, 1993), and found that Rap1B mRNA expression was constitutive in both normal and malignant melanocytes, and was not affected by FK228.

It has been reported that Rap1A/Krev-1 inhibits Ras-mediated ERK activation via competitive interference with c-Raf kinase as an antagonist of Ras (Kitayama *et al*., 1989; Cook *et al*., 1993; Hu *et al*., 1997). We therefore examined the expression and activation status of the components of the Ras–Raf–MEK1/2–ERK1/2 pathway in FK228-treated melanoma cells by immunoblotting using activation-state antibodies. First, we confirmed the upregulation of Rap1 at the protein level. In accord with the observed increase in mRNA expression, the amount of Rap1 protein was increased by FK228 in both a dose- and a time-dependent manner (Figure 2b). The upregulation of Rap1 was accompanied by a decrease in the phosphorylated/activated forms of c-Raf, MEK1/2, and ERK1/2, whereas the total amounts of these proteins and B-Raf did not change (Figure 2b, and data not shown). In addition, FK228 decreased the expression of $p21^{Ras}$ in melanoma cells. The down-regulation of Ras was considered to be translational or post-translational, because FK228 did not reduce the abundance of the Ras transcript (Figure 2c). Other members of MAP kinase pathways, such as p38 MAP kinase and SAPK/JNK, were not activated in the melanoma cell lines used in our study (data not shown).

In addition, we performed a similar analysis using normal melanocytes, which are relatively resistant to the drug. As shown in Figure 2d, Rap1 protein was only marginally increased in FK228-treated normal melanocytes, which is compatible with the results of Northern blotting. FK228 induced a decrease in the level of phosphorylated ERK1/2 in normal melanocytes less than that in melanoma cells; the reduction rates after normalization to β-actin levels are 56.0% in normal melanocytes (Figure 2d) and 83.4% in MM-LH cells (Figure 2b) at 24 h of culture with FK228. This

reduction is well correlated with the decrease in BrdU incorporation, suggesting that FK228-mediated growth suppression is closely associated with the modulation of Rap1/Ras–ERK1/2 signaling components.

Cytotoxic effects of FK228 are at least in part mediated by the upregulation of Rap1 in melanoma cells

To determine whether the inhibition of Ras–Raf–ERK1/2 signaling was a direct effect of FK228 or was mediated by Rap1, we examined the effects of exogenous Rap1 overexpression on cell viability and the activation status of Ras–MAP kinase cascade components. Forced expression of both wild-type and activated Rap1 (Kitayama *et al.*, 1990) resulted in an increase in the size of the sub-G1 fraction (Figure 3a) and a decrease in phosphorylated/activated ERK1/2 (Figure 3b) in MM-LH cells, suggesting that the upregulation of Rap1 *per se* can confer a suppression of MAP kinase activity, thereby leading melanoma cells to apoptosis. Unexpectedly, Ras expression was suppressed by exogenous Rap1 (Figure 3b), raising the possibility that Rap1 also mediates the downregulation of Ras in FK228-treated melanoma cells. However, the involvement of other factors, such as other 'FK228 effector genes', is highly likely, because the magnitude of apoptosis observed here is lower than that of FK 228-treated cells: approximately 40% in Rap1-overexpressing cells (Figure 3a) vs more than 50% in FK228-treated cells (Figure 1d).

To further corroborate the role of Rap1 in the cytotoxic activity of FK228, we attempted to abrogate the drug effect by interfering with the upregulation of Rap1 with small interfering RNA (siRNA). As shown in Figure 4a and b, siRNA against Rap1, but not control siRNA, effectively blocked the FK228-induced increase in Rap1. In the presence of Rap1 siRNA, FK228 was unable to induce either apoptosis (Table 2) or the inactivation of ERK1/2 (Figure 4c) in MM-LH cells. In addition, the downregulation of Ras was also canceled by Rap1 siRNA (data not shown), suggesting the causal relationship between Rap1 induction and Ras suppression. Taken together, these results indicate that the cytotoxicity of FK228 is at least in part mediated by the upregulation of Rap1.

Rap1 is an endogenous regulator of the Ras–MAP kinase signaling pathway in melanoma cells

Recent investigations have revealed that the abnormalities among Raf family members, such as activating mutations in the BRAF gene and c-Raf hyperactivity, are observed in most patients with malignant melanoma (Hubbard, 2004; Wan *et al.*, 2004). We therefore examined the presence of these abnormalities and their respective relationships to Rap1 in melanoma cell lines. T1796A substitution of the BRAF gene, which results in a V599E amino-acid change, was detected in two of the six cell lines used in this study (MM-Ac and MM-RU), whereas no mutations were detected in other portions of exon 15, nor anywhere in exon 11 (data not shown). The hyperactivity of c-Raf kinase, as judged by increased autophosphorylation, was observed in the MM-LH cell line (data not shown). As a result of these abnormalities, ERK1/2 was constitutively activated in MM-Ac, MM-RU, and MM-LH cell lines (Figure 5a). Despite the absence of known mutations, ERK1/2 was also hyperphosphorylated in three other cell lines, as compared to that in normal melanocytes, suggesting that the deregulation of the Ras–MAP kinase cascade is universally

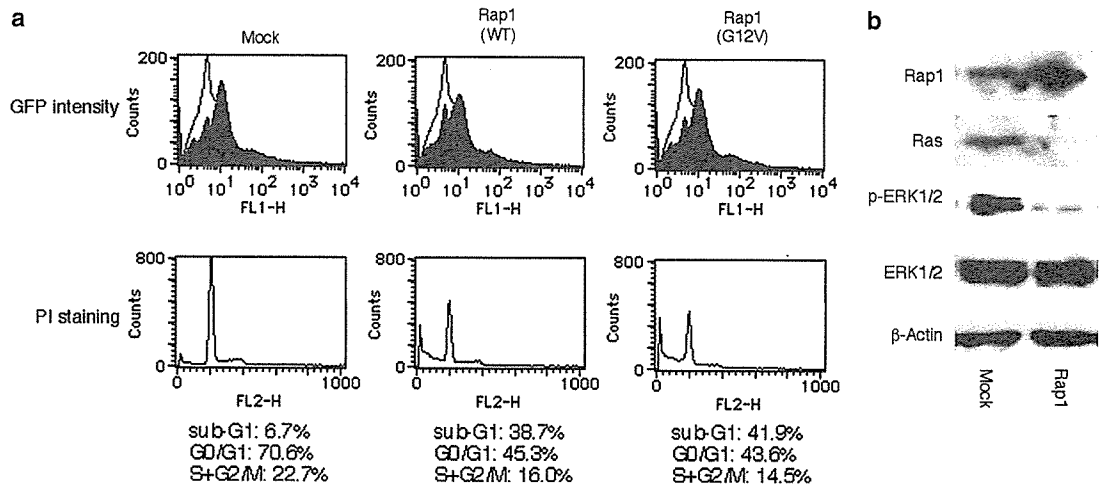

Figure 3 Effects of Rap1 overexpression on cell viability and ERK1/2 phosphorylation. (a) MM-LH cells were transfected with 2 μg of either an empty pcDNA 3.1 vector (Mock), a pcDNA 3.1 vector containing wild-type Rap1A/Krev-1 (WT), or a G12V active mutant (G12V) and 1 μg of pIRES2-EGFP vector using LipofectAMINE 2000. After 48 h, the cells were harvested and subjected to flow cytometric analysis for GFP intensity and cell cycle profile using propidium iodide (PI) staining. In the upper panel, the filled and empty lines indicate transfected cells and untreated controls, respectively. The calculated sizes of the sub-G1, G0/G1, and S + G2/M fractions are shown below each DNA histogram. (b) Whole-cell lysates were simultaneously prepared and subjected to immunoblot analysis for Rap1, Ras, phosphorylated ERK1/2, total ERK1/2, and β-actin expression.

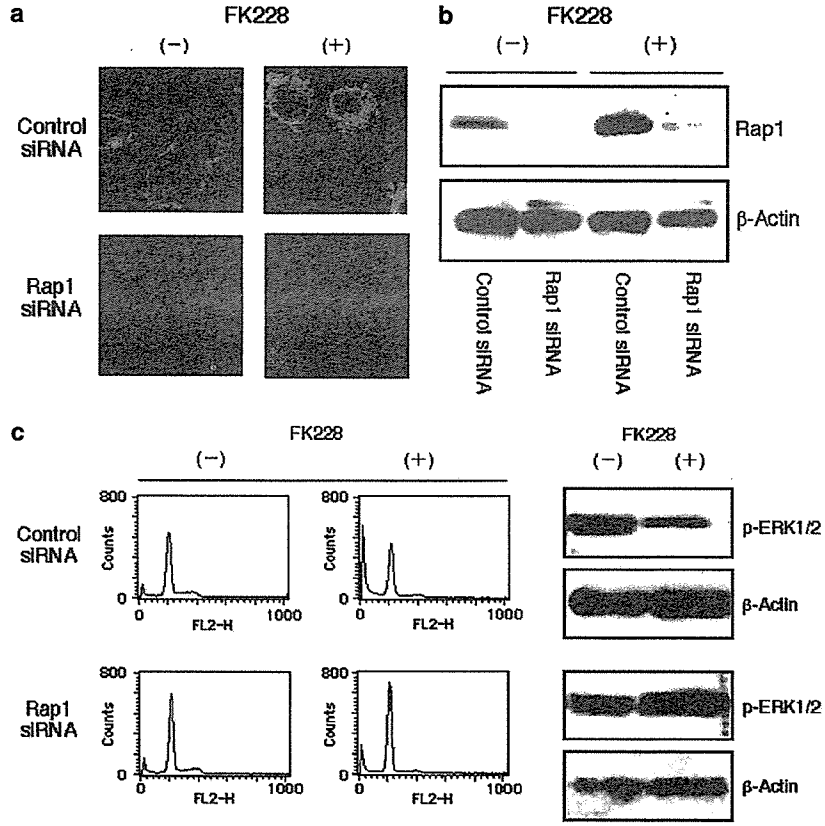

Figure 4 Effects of siRNA against Rap1 on cell viability and ERK1/2 phosphorylation. MM-LH cells were transfected with 3 μg of an equimolar mixture of either a pcPURU6βicassette vector containing TA0024-01, TA0024-02, and TA0024-03 (siRNA) or their corresponding scrambled sequences (Control). After 48 h, the cells were split into equal amounts and were respectively placed into two dishes, and FK228 was added into one of these dishes at a final concentration of 100 nM (+). After an additional 24 h of culture, the cells were stained with anti-Rap1 antibody in preparation for confocal microscopy (**a**), or subjected to immunoblotting for Rap1 expression (**b**) and ERK1/2 phosphorylation (**c**, right panel) and cell cycle analysis (**c**, left panel). β-Actin expression is shown as a loading control. The quantified results of cell cycle analysis are shown in Table 2.

Table 2 Cell cycle profile of siRNA-treated MM-LH cells

siRNA	*Cell cycle profile*[a]	*FK228*	
		(−)	*(+)*
Control siRNA	Sub-G1	13.9%	32.3%
	G0/G1	76.9%	54.8%
	S+G2/M	9.2%	12.9%
Rap1 siRNA	Sub-G1	13.7%	9.3%
	G0/G1	69.2%	73.3%
	S+G2/M	17.1%	17.4%

[a]The data shown in Figure 4c were quantified using the ModFit LT 2.0 program (Verity Software, Topsham, ME, USA).

present in melanoma cells (Figure 5a). Interestingly, the cell lines with an activating BRAF mutation were revealed to overexpress Rap1, whereas the Rap1 levels were relatively low in the other cell lines (Figure 5a). An abundance of Rap1 was negatively correlated with a sensitivity to FK228; the cell lines showing BRAF mutation/Rap1 overexpression were relatively resistant to the apoptosis-inducing effects of the drug (Figure 5b and Table 3 for quantification). This may be due to the inability of FK228 to further increase the abundance of Rap1 in these cells (Figure 5c). These results again provide support for the putative role of Rap1 as a mediator of the effects of FK228.

Finally, we attempted to elucidate the significance of Rap1 overexpression in melanoma cells with a BRAF mutation. Immunoprecipitation/immunoblot analysis revealed that Rap1 formed a complex with B-Raf in MM-RU cells, although this association was also observed in MM-LH cells lacking a BRAF mutation (Figure 6a). The complex formation was also visible on confocal microscopy in both cell lines (Figure 6b, yellow signals are indicative of colocalization). To investigate the function of endogenous Rap1 in melanoma cells, we targeted Rap1 by using siRNA. As shown in Figure 6c, the siRNA-mediated decay of Rap1 resulted in a decrease in the occurrence of spontaneous apoptosis and an increase in the number of cells in the S phase of the cell cycle among MM-RU cells. These results suggest that Rap1 acts as an endogenous suppressor of the hyperactivity of mutated B-Raf in some melanoma cells, and the presence of a feedback link between B-Raf and Rap1.

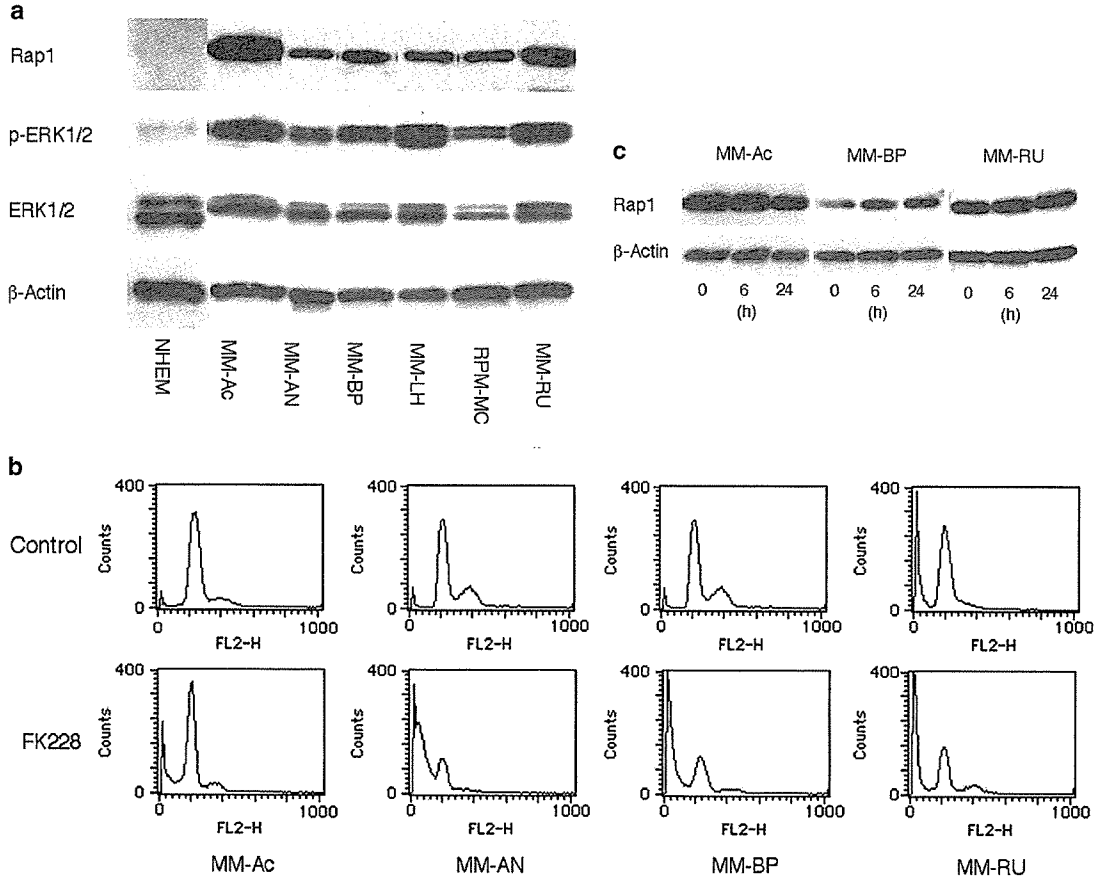

Figure 5 Expression of Rap1 and its relationship to FK228 sensitivity in melanoma cell lines. (**a**) Expression of Rap1, a phosphorylated species of ERK1/2, and ERK1/2 was examined in normal melanocytes (NHEM) and in six melanoma cell lines by immunoblotting. β-Actin expression served as a loading control. (**b**) MM-Ac, MM-AN, MM-BP, and MM-RU cells were cultured in the absence (Control) or presence (FK228) of 100 nM FK228 for 48 h, and were then subjected to flow cytometric analysis for cell cycle profiling. The quantified results are shown in Table 3. (**c**) Whole-cell lysates were prepared from MM-Ac, MM-BP, and MM-RU cells at the indicated time points, and subjected to immunoblotting for Rap1 and β-Actin expression.

Table 3 Cell cycle profile of FK228-treated melanoma cell lines

	Cell cycle profile[a]	*MM-AC*	*MM-AN*	*MM-BP*	*MM-RU*
Control	Sub-G1	4.6%	6.5%	2.4%	11.5%
	G0/G1	76.5%	67.8%	64.4%	75.1%
	S+G2/M	18.9%	25.7%	33.2%	13.4%
FK228	Sub-G1	19.3%	68.6%	57.3%	22.6%
	G0/G1	69.0%	24.2%	32.5%	54.6%
	S+G2/M	11.7%	7.2%	10.2%	22.8%

[a]The data shown in Figure 5b were quantified using the ModFit LT 2.0 program (Verity Software, Topsham, ME, USA).

Discussion

HDAC inhibitors are emerging as a new class of anticancer drugs (Melnick and Licht, 2002; Johnstone and Licht, 2003; Kim *et al.*, 2003). As the principle of their action differs from that of conventional chemotherapeutic agents, HDAC inhibitors are expected to be effective for treatment-resistant cancer including malignant melanoma. In this study, we found that the HDAC inhibitor FK228 was more effective against melanoma than other commonly used drugs such as adriamycin, vincristine, and interferon-β. FK228 almost completely suppressed cell growth and induced apoptosis in melanoma cells at $C_{max.}$, with less toxic effects on normal cells including melanocytes. These results are in line with recent studies using uveal melanoma cell lines (Klisovic *et al.*, 2003). Furthermore, we confirmed the antimelanoma effects of the drug *in vivo* using an animal model. Taken together, these findings appear to strongly encourage the clinical application of HDAC inhibitors, especially FK228, for malignant melanoma in the near future.

HDAC inhibitors are believed to exert cytotoxic effects by modulating transcription through the hyperacetylation of promoter regions. Target genes that have thus far been reported include cell cycle control elements (p21/Cip1, p27/Kip1, and cyclins A and D) (Sandor *et al.*, 2000; Derjuga *et al.*, 2001), apoptosis-inducing genes (Fas, Bax, and TNF) (Henderson *et al.*, 2003; Sutheesophon *et al.*, 2005), angiogenesis inhibitors (von

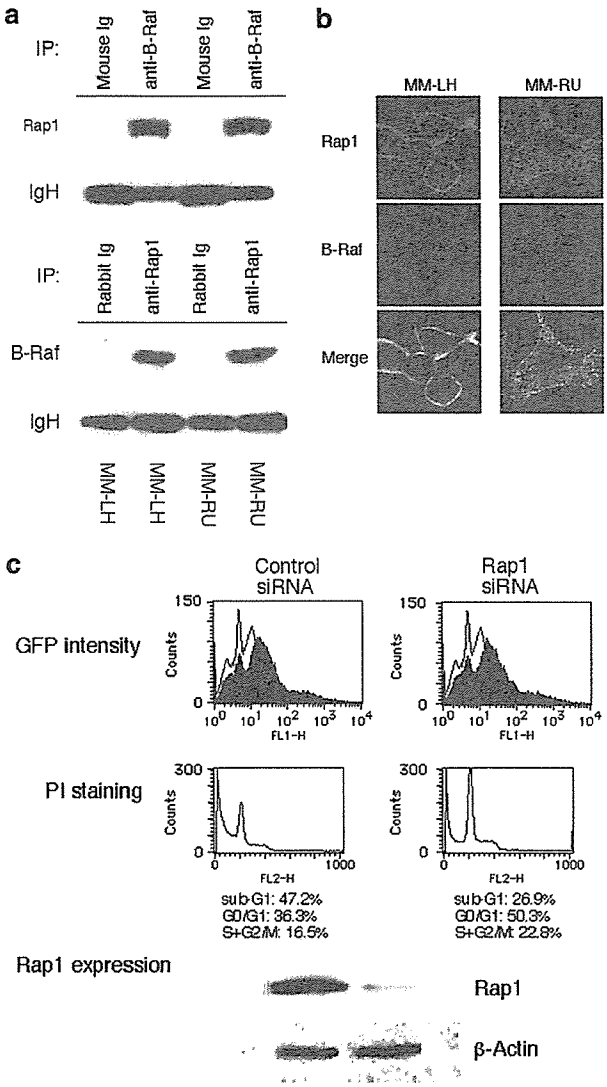

Figure 6 Intracellular association of Rap1 and B-Raf and its functional significance in melanoma cells. (**a**) Upper panel: Whole-cell lysates from MM-LH and MM-RU cells were subjected to immunoprecipitation with either preimmune mouse immunoglobulin (Mouse Ig) or anti-B-Raf monoclonal antibody, followed by immunoblotting with anti-Rap1 antibody. Lower panel: Whole-cell lysates from MM-LH and MM-RU cells were subjected to immunoprecipitation with either preimmune rabbit immunoglobulin (Rabbit Ig) or anti-Rap1 polyclonal antibody, followed by immunoblotting with anti-B-Raf antibody. Coomassie brilliant blue staining of the precipitated immunoglobulin heavy chain (IgH) is shown as a loading control. (**b**) MM-LH and MM-RU cells were double-stained with anti-Rap1 and anti-B-Raf antibodies as described in Materials and methods. (**c**) MM-RU cells were transfected with a pcPURU6βicassette vector containing either siRNA against Rap1 or a scrambled control, and were subjected to cell cycle analysis and Rap1 immunoblotting after 24 h.

Hippel-Lindau gene) (Kim *et al.*, 2001), and adhesion molecules (CD86) (Maeda *et al.*, 2000). In this study, we attempted to identify melanoma-specific target genes by comparing the gene expression profiles of melanoma cells and normal melanocytes. Seven genes fulfilled the criteria for FK228 effector genes, namely Silver-like (gp100/pMel17), TNF-α-induced protein 6, Rap1A, ADP-ribosylation factor 4, FLJ23028 (c-mer homolog), Coiled-coil forming protein 1, and TFIIB. We first pursued determination of the role of Rap1, a small GTP-binding protein of the Ras family, for two reasons. First, Rap1 is a regulator of Ras–MAP kinase signaling, which is altered in the vast majority of patients with melanoma. Second, Rap1A was originally isolated as Krev-1 by virtue of its ability to restore the malignant phenotype of activated Ras-transformed fibroblasts back to the normal phenotype (Kitayama *et al.*, 1989), which is identical to the strategy used for the discovery of FK228 (Ueda *et al.*, 1994). As anticipated, it was demonstrated that the cytotoxic effects of FK228 were at least in part mediated by the upregulation of Rap1A.

Recent investigations have revealed that abnormalities in the Ras–MAP kinase pathway are observed in most patients with malignant melanoma. Such abnormalities include activating mutations of N-Ras (4–30% of cases) (Omholt *et al.*, 2003) and BRAF (40–70%) (Davies *et al.*, 2002; Daniotti *et al.*, 2004), and c-Raf hyperactivity (10%) (Wan *et al.*, 2004). However, the significance of these abnormalities has not yet been firmly established; for example, benign melanocytic nevi is also associated with a high rate of mutation of the BRAF gene (Kumar *et al.*, 2004). Nonetheless, it is believed that constitutive activation of Ras and/or Raf family kinases bypasses the requirement of growth factors and mitogenic stimuli, and serially activates MEK1/2, ERK1/2, and target molecules such as c-Myc and cyclin D, thereby leading to the deregulated proliferation of melanocytes (Satyamoorthy *et al.*, 2003). The melanoma cell lines used in this study showed constitutive activation of this pathway via BRAF mutation in two lines, and c-Raf hyperactivation in one line. These abnormalities may be a target for therapeutic intervention, and the quest for isolation of the inhibitors of this pathway is currently underway in many laboratories (Karasarides *et al.*, 2004). In this study, we found that FK228 suppressed the Ras–Raf–MEKK1/2–ERK1/2 pathway by upregulating Rap1 and downregulating Ras expression. The results of Rap1 overexpression and siRNA intervention suggest that Rap1 plays a major role in FK228-induced apoptosis, and the downregulation of Ras is also Rap1 dependent. Further investigation is required to elucidate the molecular basis of Rap1-mediated suppression of Ras expression, although translational or post-translational mechanisms are suggested in our study.

Rap1 is a small GTP-binding protein of the Ras family with the highest homology to Ras. It has two isoforms, Rap1A and Rap1B, with 95% homology, whose functional difference remains to be determined (Bokoch, 1993; Noda, 1993). In agreement with the method of isolation, several reports have provided evidence indicating that Rap1 antagonizes Ras signaling by trapping Ras effectors, in particular c-Raf, in an inactive complex (Kitayama *et al.*, 1989; Cook *et al.*, 1993; Hu *et al.*, 1997). To date, the biological functions of Rap1 have been divided into two categories: (1) regulation of cell proliferation and (2) modulation of

integrin-mediated functions. The latter category includes cell-to-cell/extracellular matrix adhesion; cell polarity, movement, and migration; and phagocytosis (Tsukamoto *et al.*, 1999; Reedquist *et al.*, 2000; Schmidt *et al.*, 2001). Although the modulation of integrin-mediated processes by Rap1 may be related to the anti-invasive and antiangiogenic effects of HDAC inhibitors, this is beyond the scope of the present study. We instead focus on growth regulatory aspects of Rap1.

Our findings are compatible with earlier studies suggesting that Rap1 has both antiproliferative and antioncogenic potential (Kitayama *et al.*, 1989; Cook *et al.*, 1993; Hu *et al.*, 1997). In melanoma cells lacking BRAF mutation, FK228 easily suppressed the activation of Ras–MAP kinase signaling through the upregulation of Rap1, which in turn resulted in cell death. In contrast, the apoptosis-inducing effect of FK228 was relatively weak in melanoma cells with BRAF mutation, probably because of the high level of endogenous Rap1 expression. The present experiments with siRNA suggested that endogenous Rap1 acted to inhibit cell proliferation and viability by suppressing deregulated B-Raf activity. This finding appears to be somewhat contradictory to previous reports in which Rap1 was implicated in the activation of the ERK pathway by the direct binding and activation of B-Raf (Vossler *et al.*, 1997; York *et al.*, 1998). However, this observation was obtained in neuronal cells treated with cAMP, and was not reproduced in other cell types. For instance, cAMP-induced ERK activation is mediated by Ras rather than by Rap1 in melanocytes (Busca *et al.*, 2000). The function of Rap1 is therefore cell context dependent, and is determined by various factors. Growth regulation by Rap1 also varies according to cell type. For example, forced expression of Rap1A in normal T-cell clones induces an anergic state with compromised ERK1/2 activation in response to antigens (Boussiotis *et al.*, 1997; Katagiri *et al.*, 2002). In addition, D'Silva *et al.* (2003) reported that Rap1 expression increased during the growth arrest and differentiation of human keratinocytes, and the inactivation of Rap1 due to rapGAP overexpression resulted in enhanced proliferation. Loss-of-function mutations of DOCK-4, a specific Rap1 activator, have been detected in various human and murine tumor cells, suggesting that impaired activation of Rap1 can account for the overgrowth and invasive properties of some cancers (Yajnik *et al.*, 2003). In contrast, mice deficient for SPA-1, a member of the SPA-1 family Rap1 GAPs, develop an abnormal proliferation of myeloid cells resembling chronic myeloid leukemia (Ishida *et al.*, 2003). These results reinforce the notion that the role of Rap1 in cell proliferation is highly cell context dependent. Furthermore, some studies have suggested that Rap1B enhances cell growth upon overexpression (Altschuler and Ribeiro-Neto, 1998; Ribeiro-Neto *et al.*, 2002). It is possible that Rap1B acts in favor of cell proliferation, whereas Rap1A impairs cell growth and viability. Therefore, the balance between Rap1A and Rap1B may be important for cellular homeostasis, and the perturbation of this balance by the upregulation of Rap1A may be an underlying mechanism of the effects of FK228. We are currently conducting further experiments in order to evaluate this hypothesis.

Materials and methods

Cell lines and cell culture

The human melanoma cell lines MM-AN, MM-BP, MM-LH, MM-RU, and RPM-MC were kindly provided by Dr H Randolph Byers (Harvard Medical School). All cell lines were established from metastatic lymph nodes, except for RPM-MC, which originated in a recurrent primary lesion (Byers *et al.*, 1991). These cell lines were maintained in minimal essential medium (MEM) supplemented with 10% fetal calf serum (FCS), penicillin G, and streptomycin sulfate. MM-Ac (a gift of Dr Hiroshi Katayama, Katayama Dermatology Clinic, Gunma, Japan) was maintained in Dulbecco's modified Eagle's medium (DMEM) supplemented with 10% FCS, penicillin G, and streptomycin sulfate.

NHEM were purchased from Kurabo Biomedicals (Osaka, Japan), and grown in Medium154S supplemented with 10% FCS, basic fibroblast growth factor, hydrocortisone, insulin, transferrin, phorbol myristate acetate, heparin, and bovine pituitary extracts (Swope *et al.*, 1995). All cultures were carried out in a 5% CO_2 and 95% air humidified atmosphere at 37°C.

Animal experiments

Male C. B-17/Icr-SCID mice (6 weeks old) were purchased from CREA Japan Inc. (Tokyo, Japan) and maintained in containment level 2 cabinets with autoclaved food and water. MM-LH cells in exponential growth phase were harvested by trypsinization, and washed twice in PBS prior to injection. Animals were treated with anti-asialo GM1 antibody (Wako, Osaka, Japan) (200 μg/body) 1 day before tumor implantation, and 1×10^7 cells were injected subcutaneously into the abdominal skin of mice. After tumors were palpable (at day 6), animals were treated with either PBS or FK228 (0.5 mg/kg, intraperitoneally, every other day) (Skov *et al.*, 2003). Tumor growth was monitored by measurement of the two maximum perpendicular tumor diameters. All experiments in this study were performed in accordance with the Jichi Medical School Guide for Laboratory Animals.

Cell proliferation assays

Cells were harvested with trypsin, and resuspended in fresh medium containing the following test drugs: interferon-β, vincristine, adriamycin, and FK228. These drugs were provided by Mochida Pharmaceutical Co. (Tokyo, Japan), Shionogi Pharmaceutical Co. (Tokyo, Japan), Kyowa Hakko Co. (Osaka, Japan), and Fujisawa Pharmaceutical Co. (Osaka, Japan), respectively. An aliquot of 100 μl was placed in each well of 96-well plates, and the plates were then incubated at 37°C for 72 h. Cell proliferation was quantitatively assessed by BrdU incorporation using a BrdU assay kit (Roche Diagnostics, Mannheim, Germany).

Cell cycle analysis

The cell cycle profile was obtained by staining DNA with propidium iodide in preparation for flow cytometry analysis with the FACScan/CellQuest system (Becton-Dickinson, San Jose, CA, USA). The size of the sub-G1, G0/G1, and S + G2/M fractions was calculated as a percentage by analysing the DNA histograms using the ModFitLT 2.0 program (Verity Software, Topsham, ME, USA).

In situ *detection of apoptosis*
Apoptosis was detected *in situ* by TUNEL analysis using a MEBSTAIN apoptosis detection kit (MBL, Nagoya, Japan). The 3′-end of fragmented DNA of apoptotic cells was labeled with dUTP-FITC, giving off focal green fluorescent signals in the nuclei.

Plasmids and transfection
Rap1/Krev-1 expression plasmids, wild-type Rap1/Krev-1 and G12V active mutant, were constructed by inserting the corresponding full-length cDNAs into a pcDNA 3.1 vector (Invitrogen, Carlsbad, CA, USA). The G12V mutant is known to suppress the activity of Ras more efficiently than wild-type Rap1/Krev1 in some cell types (Kitayama *et al.*, 1990). An empty pcDNA 3.1 vector was used as a control. siRNA against Rap1 was subcloned into the pcPURU6βicassette siRNA expression vector (Takara Bio Co. Ltd, Shiga, Japan), expanded, and purified with an EndoFree plasmid purification kit (Qiagen Inc., Valencia, CA, USA). The target sequences of siRNA are as follows; TA0024-01, AGTCAAAGATCAA TGTTAA (nt 758); TA0024-02, AGCAGAAGATCGTCAG TAT (nt 278); TA0024-03, AGATCAATGTTAATGA GAT (nt 764). We used the scrambled sequences of each siRNA as controls. Transfection was carried out using LipofectAMINE 2000 transfection reagent (Invitrogen) according to the manufacturer's instructions. Transfection efficiency was assessed by cotransfection of the green fluorescent protein (GFP) expression vector pIRES2-EGFP (Clontech, Palo Alto, CA, USA). Upon flow cytometry and visual inspection, 20–30% of cells were found to be successfully transfected without significant variation among samples (data not shown).

Screening of the gene expression profile by DNA chip analysis
We cultured melanoma cell lines and NHEM in the absence or presence of 100 nM FK228 for 6 h, and isolated poly(A) RNA using a Poly(A) Quik mRNA isolation kit (Stratagene, La Jolla, CA, USA). Poly(A) RNAs from FK228-treated cells and the untreated control were labeled with Cy5 and Cy3, respectively, and hybridized to IntelliGene II human CHIP version 1.0 (Takara), which contains cDNA fragments of 3893 human cancer-related and cytokine genes. Precise information about the array is available at the manufacturer's website (http://www.takara.com). The cDNA array was scanned at 560 nm using the Affimetrix 428 Array Scanner, and the expression value for each gene was calculated as the average intensity difference using BioDiscovery ImaGene version 4.2 software. Expression values were normalized across the sample set by scaling the average of the fluorescent intensities of all genes on the array (Ferrando *et al.*, 2002).

Northern blotting
Total RNA was extracted from cells using an Isogen RNA extraction reagent (Nippon Gene, Toyama, Japan). A 15 μg portion of RNA samples was denatured with formaldehyde, and electrophoresed in a formaldehyde-agarose gel. RNA was then transferred onto nylon filters, and hybridized with Rap1A (Krev-1), Rap1B, and H-Ras cDNA probes, which were labeled with [^{32}P]dCTP using the Megaprime DNA labeling system (Amersham Pharmacia Biotech., Buckinghamshire, England), in Rapid-hyb buffer (Amersham Pharmacia Biotech.) for 1 h. The filters were washed once in 2 × SSC and 0.1% SDS at room temperature (RT) for 20 min, and three times in 0.1 × SSC and 0.1% SDS at 65°C for 15 min before being subjected to autoradiography. The signal intensities were quantified by densitometer.

Rap1A, Rap1B, and H-Ras cDNA fragments were prepared by PCR using the following primer pairs (D'Silva *et al.*, 2003): Rap1A (Krev-1), sense 5′-AATGTGACCTGGAAGATGAG CG-3′ and antisense 5′-AGGCAACAGTTCTTCATTCC-3′; Rap1B, sense 5′-TAGTCGTTCTTGGCTCAGGAGG-3′ and antisense 5′-AATGTGGACTGTGCTGTGATGG-3′; H-Ras, sense 5′-GGAAGCAGGTGGTCATTGATGG-3′ and antisense 5′-AGATTCCACAGTGCGTGC-3′. After 35 cycles of amplification at an annealing temperature of 60°C, PCR products were purified with a Wizard SV gel and PCR clean-up system (Promega, Madison, WI, USA).

Western blotting
For preparation of protein samples, cells were washed once with ice-cold phosphate-buffered saline, and were lysed on ice in cell lysis buffer (50 mM Tris-HCl, pH 8.0, 120 mM $NaCl_2$, 0.5% Nonidet P-40, 100 mM sodium fluoride, and 200 μM sodium orthovanadate) containing protease inhibitors. The particles were pelleted by centrifugation at 14 500 *g* for 15 min at 4°C. The supernatants were collected, and the protein contents were measured using a Bio-Rad protein assay kit (Bio-Rad, Richmond, CA, USA). Equal amounts of protein samples (20–40 μg) were electrophoresed on 10% SDS–polyacrylamide gels, and were then transferred onto Immobilon-P membranes (Millipore Corporation, Bedford, MA, USA). The membranes were incubated in 10% nonfat dry milk and 1% bovine serum albumin in Tris-buffered saline containing 0.05% Tween 20 (TBS-T) for 1 h at RT in order to avoid nonspecific protein binding. The membranes were placed in primary antibody solution for 1 h at RT or overnight at 4°C, depending on the antibody. The following primary antibodies were used: anti-Rap1 (121; Santa Cruz Biotechnology, Santa Cruz, CA, USA), anti-p21^{Ras} (clone 18; BD Transduction Laboratories, Lexington, KY, USA), anti-B-Raf (F-7; Santa Cruz Biotechnology), anti-phosphorylated c-Raf (Ser259) (Cell Signaling Technology, Beverley, MA, USA), anti-phosphorylated MEK1/2 (Ser217/221) (Cell Signaling Technology), anti-phosphorylated ERK1/2 (Thr202/Tyr204) (Cell Signaling Technology), anti-ERK1/2 (Cell Signaling Technology), anti-phosphorylated p38 MAP kinase (Thr180/Tyr182) (Cell Signaling Technology), anti-phosphorylated JNK (Thr183/Tyr185) (Cell Signaling Technology), and anti-β-actin (C4; ICN Biomedicals, Aurora, OH, USA). We used anti-rabbit or anti-mouse IgG linked to horseradish peroxidase (Amersham Corporation) as the second antibody, and an ECL enhanced chemiluminescence system (Amersham Corporation) for detection.

Immunoprecipitation/immunoblotting assays
After being precleared with protein G-Sepharose, whole-cell lysates (300 μg) were incubated with 2 μg of either anti-B-Raf antibody (F-7) or mouse IgG in 200 μl of cell lysis buffer. After brief centrifugation, the supernatants were rocked overnight at 4°C in the presence of protein G-Sepharose beads. Immune complexes were collected on the beads, washed three times in cell lysis buffer, and applied to 10% SDS–PAGE, followed by immunoblotting with anti-Rap1 antibody (sc-65). Reciprocal experiments were carried out according to the same protocol except that protein A-Sepharose and rabbit IgG were used instead of protein G-Sepharose and mouse IgG, respectively.

Confocal laser microscopy
The entire procedure was performed as described previously (Furukawa *et al.*, 2002). The cells were collected on glass slides using a Cytospin centrifugator (Shandon Scientific, Cheshire, UK), and fixed in 4% paraformaldehyde in PBS. Rap1 was